

Combining Information Across Diverse Sources: The II-CC-FF Paradigm

June 2020

Céline Cunen and Nils Lid Hjort

¹Department of Mathematics, University of Oslo

Abstract

We introduce and develop a general paradigm for combining information across diverse data sources. In broad terms, suppose ϕ is a parameter of interest, built up via components ψ_1, \dots, ψ_k from data sources $1, \dots, k$. The proposed scheme has three steps. First, the Independent Inspection (II) step amounts to investigating each separate data source, translating statistical information to a confidence distribution $C_j(\psi_j)$ for the relevant focus parameter ψ_j associated with data source j . Second, Confidence Conversion (CC) techniques are used to translate the confidence distributions to confidence log-likelihood functions, say $\ell_{\text{conv},j}(\psi_j)$. Finally, the Focused Fusion (FF) step uses relevant and context-driven techniques to construct a confidence distribution for the primary focus parameter $\phi = \phi(\psi_1, \dots, \psi_k)$, acting on the combined confidence log-likelihood. In traditional setups, the II-CC-FF strategy amounts to versions of meta-analysis, and turns out to be competitive against state-of-the-art methods. Its potential lies in applications to harder problems, however. Illustrations are presented, related to actual applications.

Key words: combining information, confidence distributions, confidence likelihoods, focused fusion, hard and soft data, meta-analysis.

1 Combining information and the II-CC-FF scheme

Our paper concerns the statistical task of combining information across different and perhaps very diverse data sources. This is of course a long-standing theme in statistics, with papers going back to Karl Pearson (cf. Simpson & Pearson (1904)); see Schweder & Hjort (2016, Ch. 13) for background and a general discussion of themes traditionally sorted under the bag-word meta-analysis, along with further basic references. The present paper aims at proposing and developing a certain paradigm, which we call the II-CC-FF method, meant to be powerfully applicable for ranges of situations far beyond the usual simpler setups. We will explain the role and nature of the Independent Inspection (II), Confidence Conversion (CC), Focused Fusion (FF) steps below.

A special case worth considering first is the textbook setup where y_1, \dots, y_k are independent estimators of the same quantity ψ , and where $y_j \sim N(\psi, \sigma_j^2)$, with known standard deviations σ_j .

An easy exercise in minimising variances shows that the optimally balanced overall estimator is

$$\hat{\psi} = \frac{\sum_{j=1}^k y_j / \sigma_j^2}{\sum_{j=1}^k 1 / \sigma_j^2} \sim N\left(\psi, \left(\sum_{j=1}^k 1 / \sigma_j^2\right)^{-1}\right). \quad (1.1)$$

A natural extension, though harder to analyse to full satisfaction, is when $y_j \sim N(\psi_j, \sigma_j^2)$, with the individual means ψ_j differing according to a $N(\psi_0, \tau^2)$ distribution. For this type of random effects model, one wishes clear inference strategies for both the overall mean ψ_0 and level of variation τ . We return to this particular problem in Sections 6.1, 8.1, and 9.1.

Many problems of modern statistics involving combining information are much more complicated than the situations sketched above, however. Sometimes one needs to combine ‘hard’ data, with clear measurements from controlled experiments, etc., with ‘soft’ data, associated with information more loosely connected to the parameters of primary interest, perhaps via measurement errors or surrogate variables. In addition there might be prior distributions available, via subject matter experts, but only for some of the parameters at play, not enough to make it into a clear Bayesian analysis. For our development of II-CC-FF we have attempted to think fundamentally and generally about combination of information problems. Our framework encompasses known meta-analysis methods, but we aim at tackling new and more challenging problems as well. Parts of the meta-analysis literature are quite narrow, with specific methods for specific problems. In that light we hope our more general approach will be useful.

In reasonably general terms, assume there is a parameter ϕ of clear interest, related to parameters ψ_1, \dots, ψ_k , either via a deterministic function $\phi = \phi(\psi_1, \dots, \psi_k)$ or via some type of random effect distribution, where such a ϕ might be a parameter related to a background distribution of the ψ_j . Suppose further that data source y_j provides information pertaining to ψ_j . For the sake of clear presentation, we let the ψ_j be one-dimensional here. Our II-CC-FF approach for reaching inference statements for the overall focus parameter ϕ can then be schematically set up as follows:

- ◊ II, *Independent Inspection*: Data source y_j is used, via appropriate models and analyses, to yield a confidence distribution $C_j(\psi_j, y_j)$ for the main interest parameter associated with study j .
- ◊ CC, *Confidence Conversion*: The confidence distribution is converted into a log-likelihood function for this main parameter of interest for study j , say $\ell_{\text{conv},j}(\psi_j)$.
- ◊ FF, *Focused Fusion*: In the fixed effect case, the combined confidence log-likelihood function $\ell_{\text{fus}}(\psi_1, \dots, \psi_k) = \sum_{j=1}^k \ell_{\text{conv},j}(\psi_j)$ is used to reach focused fusion inference for $\phi = \phi(\psi_1, \dots, \psi_k)$. With random effects, the fusion involves the computation of an integral.

We do make use of certain subscripts in our paper, meant as helpful signposting. The subscript ‘conv’ is for likelihood functions coming out the CC-step; ‘fus’ relates to the FF-step; while ‘prof’ and ‘cprof’ are used for the profile log-likelihood and its corrected version (see Section 5.2).

The extent to which some or all of these steps will be relatively straightforward or rather complicated to carry out depends to a high degree on the special features of the given source combination problem. The steps are not ‘isolated’ or fully separated, but often related. In Section 5.1 we provide a standardised version of II-CC-FF, with a generic recipe to follow, but we will see that in many cases one could or should be more careful about the various steps. In situations where the statistician has all the raw data and the particular models used for analysing the different sources of

information, the CC step is in a conceptual sense not difficult, as the required log-likelihood parts may be worked out from first principles. In various situations confronting the modern statistician this is rather more difficult, however, as one might have to base one's analysis on summary measures, directly or indirectly given via other people's work, reports and publications. The II-CC-FF paradigm is meant to be powerfully applicable in such situations too.

A pertinent question is whether or why there is a need for specific methods for combination of information in the first place; in a suitable sense, all of statistics concerns combination of information. One might therefore ask why there even exist subfields such as meta-analysis, and specific framework aimed at combination of information such as our own. So isn't meta-analysis just analysis? Two related responses are as follows. (i) Sometimes the full sets of data are not available, with access only to summaries or partial summaries. Issues here are storage, the practicalities of other people's files, privacy concerns, etc. (ii) Sometimes it might be easier, conceptually or practically, to analyse the different sources or studies separately first, and then combine these pieces of summarised information. Also, a statistical prediction is that modern statistics to an increasing degree will be concerned with such issues and challenges, finding and organising bits and pieces of information across different sources, with a need to reach conclusions based on these pieces.

After a motivating illustration, below, we start in Section 2 with a brief review of confidence distributions (CDs), which are essential for the Independent Inspection (II) part of the programme. We then proceed with giving details related to the basics of Confidence Conversion (CC) in Section 3 and Focused Fusion (FF) in Section 4. In Section 5 we provide a standard version of our II-CC-FF framework, and investigate some pitfalls and solutions. In Section 6 we investigate the use of our II-CC-FF scheme in well-established meta-analysis situations, and in Section 7 connections with other CD based approaches are explored. Further performance and comparison issues are examined in Section 8, both via simulations and decision theoretic risk functions. There, we find that II-CC-FF methods are competitive in several traditional meta-analysis settings. The three step II-CC-FF machinery is then seen in action through four applications laid out in Section 9.

Motivating illustration

The following concrete illustration, which has certain features placing it outside the usual meta-analysis setups and methods, shows the three steps of the II-CC-FF at work, but with a minimum of details. The nonstandard aspect for this illustration is partly that different studies of the same statistical question have reported different summary measures – six studies (call them type A) have reported summary statistics based on continuous outcomes, while five other studies (which we call type B) reported summaries based on a binary outcome. More crucially, the focus parameter β in question, a regression coefficient related to the difference between treatments, is not identifiable, and hence cannot be estimated directly, for the type B studies. In fact, these type B studies only inform us about a certain β/σ , where also σ is not identifiable, or estimable, from those studies. Also, the raw data, for these studies, are not available. The data employed here were first analysed in Whitehead et al. (1999); related problems have been treated in Dominici & Parmigiani (2000) and Liu et al. (2015).

We have eleven randomised trials investigating the use of oxytocic drugs during labour and its potential effect on postpartum blood loss. Each study has two groups of patients, a treatment group receiving oxytocic drug and a control group receiving no drugs of that type. Taking $y_{i,j}$ to

be the blood loss for patient i in study j , we may use the simple model $y_{i,j} = \alpha_j + \beta z_{i,j} + \varepsilon_{i,j}$, with the $\varepsilon_{i,j}$ independent and $N(0, \sigma^2)$, and with $z_{i,j}$ an indicator variable, equal to 0 for patients in the control group and 1 for patients in the treatment group. Here β is the treatment effect and the parameter of main interest.

For the six type A trials, we have the mean and the empirical standard deviation of the blood loss in the two groups of patients. With the simple normal model above, these four summary statistics are sufficient for each trial, and we thus have access to the full log-likelihood $\ell_{A,j}(\beta, \alpha_j, \sigma)$ for each continuous trial j . For the five type B trials, however, we merely have counts of the number of patients in each group having a blood loss of more or less than 500 ml. These numbers constitute a non-sufficient summary; we thus have less information in these studies compared to the continuous ones, and log-likelihood functions not able to inform on β directly, only on β/σ . More specifically, based on the normal model above, we obtain a probit-type log-likelihood for these binary trials, say $\ell_{B,j}(\theta, \gamma_j)$, with $\gamma_j = (500 - \alpha_j)/\sigma$ and $\theta = \beta/\sigma$.

Having made these modelling assumptions, the steps in the II-CC-FF recipe follow straightforwardly. Using the log-likelihood functions described above, we can, by methods described in the next section, construct *confidence curves* for the parameter of interest for each of the studies.

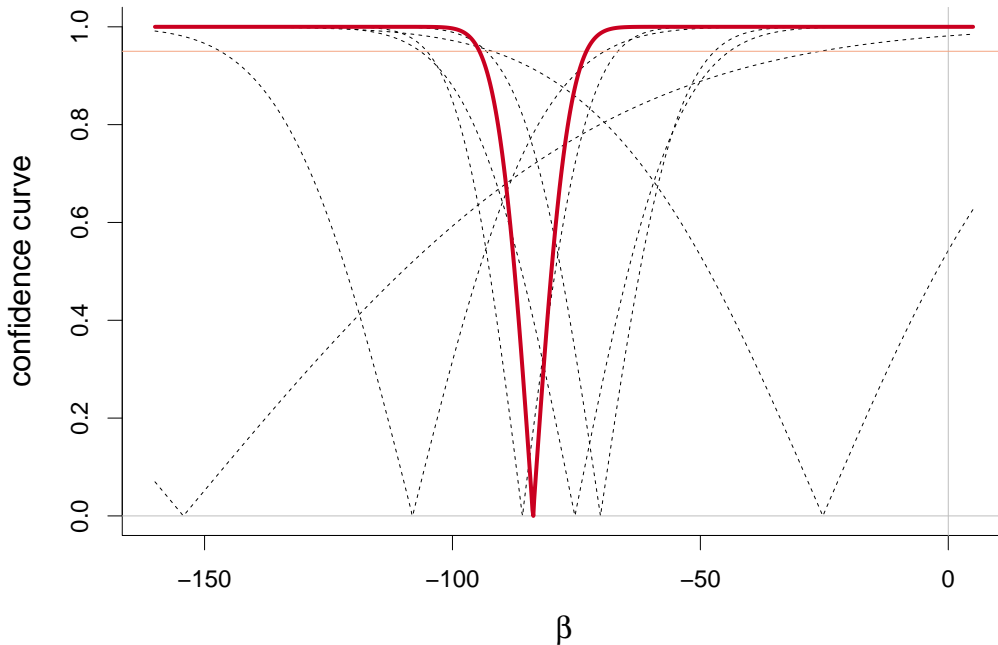


Figure 1.1: Confidence curves for the treatment effect in the six continuous trials (dashed, black). In red, the confidence curve combining all the eleven studies. The horizontal red line marks the 95% confidence level. The median confidence estimate is -83.7 ml, with 95% interval $[-94.4, -73.1]$.

The CC step is simple in this case, with no extra work required, since the log-likelihood functions were used in the construction of the confidence curves for each study. In other situations we might have to carry out the conversion from confidence statements to log-likelihood functions in ways described in Section 3. Via arguments explained in more detail in the next section, we reach log-likelihood contributions $\ell_{A,\text{prof},j}(\beta, \sigma)$ for the continuous studies and $\ell_{B,\text{prof},j}(\beta/\sigma)$ for

the binary studies. In the FF step these are summed, to reach

$$\text{FF: } \ell_{\text{fus}}(\beta, \sigma) = \sum_{j=1}^6 \ell_{A,\text{prof},j}(\beta, \sigma) + \sum_{j=1}^5 \ell_{B,\text{prof},j}(\beta/\sigma).$$

Next we profile out σ and obtain the final combined confidence curve by

$$\text{cc}^*(\beta, \text{all data}) = \Gamma_1(2\{\max \ell_{\text{fus}}(\beta, \hat{\sigma}(\beta)) - \ell_{\text{fus}}(\beta, \hat{\sigma}(\beta))\}),$$

with $\Gamma_1(\cdot)$ the c.d.f. of a χ_1^2 . In Figure 1.1, the thick red curve is this combined confidence curve. It is clearly narrower than all the individual curves and placed roughly in the middle of them, as we would expect.

The combined inference clearly demonstrates that oxytocic drugs reduce postpartum blood loss, which is in agreement with the conclusions in Whitehead et al. (1999). Here we have zoomed in on β as the focus parameter, to pinpoint precisely how much the two groups differ in blood loss. For clinicians it might be of more direct interest to consider the probabilities for having a postpartum blood loss greater than a threshold, like 500 ml, for the two groups, and then focus on the odds ratio, say ρ . Our approach can easily accommodate such an analysis too, with ρ rather than β in the FF step, yielding a figure similar to Figure 1.1, but now for ρ . The II, CC, FF steps are not intended to form a unique recipe, as there are individual variations, depending on the application at hand. In the FF step above the log-likelihood contributions for type A and type B information were arrived at via profiling of the fuller log-likelihoods constructed under the auspices of the regression model we started out with. In other applications this would not be possible, and there would be a need to convert CC information to log-likelihoods, a theme we examine in Section 3.

2 Independent Inspection: confidence distributions

Suppose Y_j denotes a set of random observations from data source j , stemming from a model with parameter θ_j , typically multidimensional, and with $\psi_j = \psi(\theta_j)$. For the ease of presentation, we let ψ_j be a one-dimensional focus parameter for now, but in general combination situations it will typically be multidimensional. A *confidence distribution* (CD) $C_j(\psi_j, y_j)$ for this focus parameter from source j has the properties (i) it is a cumulative distribution function (c.d.f.) in ψ_j , for each y_j , and (ii) at the true value θ_0 , with associated true value $\psi_0 = \psi(\theta_0)$, the distribution of $C_j(\psi_0, Y_j)$ is uniform on the unit interval. From this follows, under standard continuity and monotonicity assumptions, that

$$P_{\theta_0}\{C_j^{-1}(0.05, Y_j) \leq \psi_0 \leq C_j^{-1}(0.95, Y_j)\} = 0.90,$$

etc., i.e. $[C_j^{-1}(0.05, y_{j,\text{obs}}), C_j^{-1}(0.95, y_{j,\text{obs}})]$ is a 90% confidence interval for ψ_j , where $y_{j,\text{obs}}$ denotes the observed dataset. Thus the CD $C_j(\psi_j, y_{j,\text{obs}})$, qua random c.d.f., is a compact and convenient representation of confidence intervals at all levels, and indeed a powerful inference summary. A close relative is the *confidence curve*, which we tend to prefer as a post-data graphical summary of information for focus parameters, defined as

$$\text{cc}_j(\psi_j, y_{j,\text{obs}}) = |1 - 2C_j(\psi_j, y_{j,\text{obs}})|. \quad (2.1)$$

It points to its cusp point, the median confidence point estimate $\hat{\psi}_{j,0.50} = C_j^{-1}(\frac{1}{2}, y_{j,\text{obs}})$, and the two roots of the equation $C(\psi_j, y_{j,\text{obs}}) = \alpha$ form a confidence interval with this confidence level.

Degrees of asymmetry are easier to spot and to convey using the confidence curve than with the cumulative CD itself; cf. illustrations in Section 9. We also note that the random $cc_j(\psi_j, Y_j)$ has a uniform distribution, at the true position in the parameter space, since $|1 - 2U|$ is uniform when U is. Indeed

$$P_{\theta_0}\{cc_j(\psi_0, Y_j) \leq \alpha\} = \alpha, \quad \text{for each } \alpha, \quad (2.2)$$

at the true parameters of the model. The confidence curve is arguably a more fundamental concept than the confidence distribution, as there are cases where a natural $cc_j(\psi_j, Y_j)$ may be constructed, with a valid (2.2), even when confidence regions are formed by disjoint intervals (as with multimodal log-likelihood functions).

For an extensive treatment of CDs, their constructions in different types of setup, properties and uses, see Schweder & Hjort (2016), and the review paper Xie & Singh (2013), with ensuing discussion contributions. The scope and broad applicability of CDs are also demonstrated in a collection of papers published in the special issue *Inference With Confidence* of the journal *Journal of Statistical Planning and Inference*, 2018 (Hjort & Schweder, 2018). Here we shall merely point to two important and broadly useful ways of constructing a confidence distribution, for a focus parameter ψ_j , based on data from a model with a multidimensional parameter θ_j . The first is to rely on an approximately normally distributed estimator, if available, say $\hat{\psi}_j \sim N(\psi_j, \kappa_j^2)$, and with standard deviation well estimated with an appropriate $\hat{\kappa}_j$. Then, with $\Phi(\cdot)$ as usual denoting the c.d.f. of the standard normal, $C_j(\psi_j, y_j) = \Phi((\psi_j - \hat{\psi}_j)/\hat{\kappa}_j)$ is an approximately correct CD, first-order large-sample correct under weak regularity conditions. In particular the estimator used can be the maximum likelihood one (ML), say $\hat{\psi}_{j,\text{ml}}$, but other estimators are allowed too in this simple construction. The second is based on the profiled log-likelihood function $\ell_{\text{prof},j}(\psi_j) = \max\{\ell_j(\theta_j) : \psi(\theta_j) = \psi_j\}$, which leads to the deviance function

$$D_j(\psi_j) = 2\{\ell_{\text{prof},j}(\hat{\psi}_{j,\text{ml}}) - \ell_{\text{prof},j}(\psi_j)\} = 2\{\ell_{\text{prof},j,\text{max}} - \ell_{\text{prof},j}(\psi_j)\}. \quad (2.3)$$

As laid out in Schweder & Hjort (2016, Chs. 2, 3), the Wilks theorem with variations then lead naturally to

$$cc_j(\psi_j, y_j) = \Gamma_1(D_j(\psi_j)), \quad (2.4)$$

with $\Gamma_\nu(\cdot)$ denoting the c.d.f. of a χ^2 with degrees of freedom ν . Typically, the second method (2.4) leads to a better calibrated confidence curve than the the simpler method mentioned first.

3 Confidence Conversion: from confidence to likelihoods

Several well-explored methods, with appropriate variations and amendments, lead from likelihood functions to CDs and confidence curves; cf. again several chapters of Schweder & Hjort (2016). Sometimes the CC step comes almost for free, in cases where the statistician can compute say log-likelihood profiles from raw data, or from sufficient statistics, for the given models. But in some cases the CC step of the II-CC-FF paradigm requires methods for going the other way, from CDs or confidence curves to log-likelihood information, and this is more involved. Among the complications is that different experimental protocols, with ensuing different CDs, might be having the same log-likelihood functions, so the link between confidence and likelihood is not one-to-one.

Schweder & Hjort (2016, Ch. 10) develop and discuss this topic at some length. For the present purposes we shall be content with what we call the *chi-squared inversion*, associated with (2.4) above. Assume that all our information about a parameter ψ_j from source j comes in the form of the confidence curve $cc_j(\psi_j, y_j)$. Then we can obtain a confidence log-likelihood contribution from source j by the following formula

$$\ell_{\text{conv},j}(\psi_j) = -\frac{1}{2}\Gamma_1^{-1}(cc_j(\psi_j, y_j)). \quad (3.1)$$

If the confidence curve has been constructed via the second general method presented in the previous section, see (2.4), we will of course simply get back the profiled log-likelihood function. The CC step therefore only comes into play when confidence curve are constructed via non-standard methods, as we will see in Applications 9.2 and 9.3, or when the only available information from source j is the confidence curve itself and we do not know exactly how it was constructed.

When a CD is available, rather than a confidence curve, one can use the *normal conversion* $\ell_{\text{conv},j}(\psi_j) = -\frac{1}{2}\{\Phi^{-1}(C_j(\psi_j, y_j))\}^2$. This is equivalent to the recipe in (3.1), when the confidence curve has been constructed via $cc_j(\psi_j, y_j) = |1 - 2C_j(\psi_j, y_j)|$. A relevant point here is that one often constructs a confidence curve $cc_j(\psi_j, y_j)$ directly, not always via (2.1), making (3.1) a more versatile tool. The normal conversion confidence likelihood is also what Efron (1993) proposed, for coming from confidence to likelihood, via different arguments and for different purposes; see also Efron & Hastie (2016, Ch. 11). For details on how well the chi-squared inversion methods works, in different scenarios, see Section 4.3.

In some situations one is able to construct a CD for source j via a one-dimensional statistics T_j , instead of using the general method from (2.4). Then one may use *exact conversion* to obtain the confidence log-likelihood. When the statistic has a continuous distribution, the exact conversion of the CD $C_j(\psi_j, T_j)$, see Schweder & Hjort (2016, Ch. 10), is $\ell_{\text{conv},j}(\psi_j) = \log |\partial C_j(\psi_j, t)/\partial t|$.

4 Focused Fusion: from full likelihood to focus parameter

Suppose now that the II and CC steps have been successfully carried out, leading to confidence log-likelihood contributions $\ell_{\text{conv},j}(\psi_j)$ from information sources $j = 1, \dots, k$. Depending on the application and its context we might then be interested in either a fixed effect approach, with the main focus parameter ϕ is a function of the ψ_j , or a random effect approach, where we introduce an additional layer of heterogeneity through a model for the ψ_j . We will treat the fixed effect case first.

4.1 Fixed effects fusion

Assuming the information sources to be independent, the overall confidence log-likelihood function is $\ell_{\text{fus}}(\psi_1, \dots, \psi_k) = \sum_{j=1}^k \ell_{\text{conv},j}(\psi_j)$. When focused inference is wished for, for a focus parameter $\phi = \phi(\psi_1, \dots, \psi_k)$, the natural way forward is, again, via profiling:

$$\ell_{\text{fus,prof}}(\phi) = \max\{\ell_{\text{fus}}(\psi_1, \dots, \psi_k) : \phi(\psi_1, \dots, \psi_k) = \phi\}.$$

By the Wilks theorem directly, or by variations of the arguments and details used to prove such theorems (cf. Schweder & Hjort (2016, Appendix)), the overall deviance function

$$D^*(\phi) = 2\{\ell_{\text{fus,prof}}(\hat{\phi}) - \ell_{\text{fus,prof}}(\phi)\}$$

tends, at the true parameter position and with increasing information volume, to a χ_1^2 . Here $\widehat{\phi}$ is the ML, maximising the profiled log-likelihood. Hence

$$cc^*(\phi, \text{all data}) = \Gamma_1(D^*(\phi)) \quad (4.1)$$

is the outcome of the three step II-CC-FF machine, a confidence curve for the focus parameter. In Section 4.3 we will come back to some discussion on the meaning of ‘increasing information volume’ in a combination context. In situations where the ψ_j represent the same focus parameter, common across sources, the scheme above simplifies.

4.2 Random effects fusion

In our II-CC-FF setting, we use the term ‘random effects’ when we wish to introduce an extra layer of heterogeneity in the fusion step. This is more easily presented when assuming that ψ_1, \dots, ψ_k are scalars. In the random effects case we do not assume that all ψ_j are equal but rather that they come from some underlying distribution. In the most canonical case, this distribution will be governed by some overall mean parameter ψ_0 and some spread parameter τ ; specifically we could have $\psi_j \sim N(\psi_0, \tau^2)$. The parameter of main interest may be either the overall mean, or the spread, or perhaps a quantile, depending on the context.

We propose the following general solution for II-CC-FF with random effects. Suppose the ψ_j are modelled as coming from a background density $f(\psi_j, \kappa)$, say, where the κ could be a centre and a spread parameter, as for (ψ_0, τ) in the normal case. Then, using the confidence log-likelihoods $\ell_{\text{conv},j}(\psi_j)$ from each source, we define the fusion log-likelihood to be

$$\ell_{\text{fus}}(\kappa) = \sum_{j=1}^k \log \left[\int \exp\{\ell_{\text{conv},j}(\psi_j)\} f(\psi_j, \kappa) d\psi_j \right]. \quad (4.2)$$

We would usually need to profile again, depending on what we are interested in, say the centre ψ_0 or spread τ for the case of a normal model for the ψ_j . To produce our final confidence curve we will often use the Wilks approximation. This II-CC-FF solution requires the computation of integrals. Sometimes numerical integration routines in R work well enough, other times we will make use of the so-called Template Model Builder package (TMB) and its Laplace approximations in order to compute the integral (Kristensen et al., 2016).

4.3 Wilks theorems for conversion and fusion

There are chi-squared approximation methods at work at sometimes several levels in our II-CC-FF scheme. For some applications the chi-squared inversion method (3.1) is crucial, as for the nonparametric CDs for quantiles in Application 9.3, and for other situations what matters more might be the chi-squared approximation of the FF step (4.1). Limit distribution results securing such χ_1^2 limits are collectively referred to as Wilks theorems, with different setups of regularity conditions. We refrain from setting up lists of precise regularity conditions here, as applications of the theory would involve different types of situations, but we give brief pointers to relevant methods and literature, as follows.

First, regarding (3.1) and conversion to log-likelihoods, both the exact log-likelihood and the inversion approximation are guaranteed to be close to the negative quadratic $-\frac{1}{2}(\psi_j - \widehat{\psi}_{j,\text{ml}})^2 / \widehat{\kappa}_j^2$, for the appropriate $\widehat{\kappa}_j$, by arguments associated with classical large-sample calculus. This would

include asymptotic normality of the ML estimator and indeed the traditional Wilks theorem, see Schweder & Hjort (2016, Ch. 2 and Appendix). The resulting approximations are typically good also when the data information volume is small, as long as the underlying models are smooth in their parameters. Second, the arguments and methods pointed to also entail that the FF inference method (4.1) is large-sample close to that of minimising the relevant $\sum_{j=1}^k (\psi_j - \hat{\psi}_{j,\text{ml}})^2 / \hat{\kappa}_j^2$ under $\phi = \phi(\psi_1, \dots, \psi_k)$ constraints. For such minimum chi-squared methods, precise Wilks theorems are given in Ferguson (1996, Section 23). Regularity conditions there are of the type where the number of information sources k is kept moderate and fixed, but with steadily more data for each. Importantly, limiting normality of estimators, along with limiting χ_1^2 results for deviances, can also be derived in the rather different setups with small data volume for each source, but where the number k increases. A case in point is where $\phi = b^t \psi$ is linear in the ψ_j , with estimator $\hat{\phi} = b^t \hat{\psi}$, and the FF step is large-sample equivalent to $D^*(\phi) = (\phi - \hat{\phi})^2 / \sum_{j=1}^k b_j^2 \hat{\kappa}_j^2$. This tends to a χ_1^2 for increasing k , under mild regularity conditions.

5 II-CC-FF versions

The overall objective of the II-CC-FF is to construct a valid confidence curve for each parameter ϕ of particular interest, typically of the form $\phi = \phi(\psi_1, \dots, \psi_k)$, incorporating the relevant information in all the sources. The framework we have presented so far has not intended to provide a single clear-cut recipe for doing such analyses in practice. Below one such concrete recipe is presented, however, which we call the standard II-CC-FF method, and which may be used for a wide range of models and data. The standard framework has limitations, which we will discuss, and which will serve as a starting point for the presentation of some partial solutions, and more fine-tuned versions of the II-CC-FF scheme. These discussions also highlight various important general issues with methods for combination of information which are relevant also outside the II-CC-FF framework.

5.1 Standard II-CC-FF

The scheme to be described now requires that we have the full data available, or sufficient summaries, from all sources. The statistical work starts by deciding on one or more parameters of particular interest, involving relevant parameters ψ_1, \dots, ψ_k from the k sources. These might be parameter vectors (i.e. need not be one-dimensional), they might differ from source to source, but may also contain common parameters across sources.

- ◊ II, *Independent Inspection*: analyse each source j separately. Assume a parametric model for the observations and put up the likelihood function. Profile out the source-specific nuisance parameters, and obtain $\ell_{\text{prof},j}(\psi_j)$.
- ◊ CC, *Confidence Conversion*: in this case we already have the log-likelihood profiles from each source, so the confidence conversion is simple, using the $\ell_{\text{prof},j}(\psi_j)$ directly.
- ◊ FF, *Focused Fusion*: here we want to obtain a confidence curve for the parameter of overall interest ϕ . Depending on the situation, (i) if ϕ is assumed to be the same across sources or a function of some source-specific parameters, sum the $\ell_{\text{conv},j}$ and then profile again if necessary; (ii) if some component of the ψ_j are assumed to come from some common distribution, use the random effects solution presented above, and then profile again if needed.

We then obtain $\ell_{\text{fus,prof}}(\phi)$, and in both cases we use the Wilks approximation to produce the final, combined confidence curve $\text{cc}^*(\phi, \text{data})$.

As for confidence curves in general, we consider the method to work if the final combined confidence curve $\text{cc}^*(\phi)$ has the right coverage properties, either exactly or approximately, as per (2.2). If the final combined confidence curve does not have the correct coverage properties, this may be due to two related problems: (1) the profiling in either the II or the FF step has gone wrong; and (2) the distribution of the deviance (based on the profile log-likelihood) is far from a χ_1^2 , i.e. the Wilks approximation is not valid.

Problem (2) is related to the issues discussed in Section 4.3 and will usually disappear when either k or the n_j increase. In situations with little data, the Wilks approximation can sometimes be ameliorated using relatively simple tools, like the Bartlett correction; see for instance Schweder & Hjort (2016, Chs. 7, 8) for a discussion on such fine-tuning methods and second-order approximations. Further, in some situations one may be able to derive and simulate the distribution of the deviance exactly, and thus bypass the use of the Wilks approximation altogether. We will see examples of such II-CC-FF versions in Sections 6.1 and 9.1.

Problem (1) is related to the profiling and the presence of nuisance parameters. In situations with nuisance parameters using the profile log-likelihood can lead to “inefficient and even inconsistent estimates” (McCullagh & Tibshirani, 1990). As we see above, the standard II-CC-FF method may often require two rounds of profiling: first in the II step where we might profile out the *source-specific* nuisance parameters, and sometimes in the FF step where we might profile out *shared* nuisance parameters (which are shared by the k sources). If we have ‘large sources’, i.e. the sample size n_j of each source is large, we can safely profile in the II step. If some or all the sources are small, however, one should be more careful. Specifically, the profiling might go wrong and we illustrate this situation with a famous example in Appendix C, the Neyman-Scott problem.

Shared nuisance parameters can be of different kinds, and here we will particularly concern ourselves with nuisance parameters arising from the random effect distribution in the FF step. For example, if we have $\psi_j \sim N(\psi_0, \tau^2)$ and our focus parameter is ψ_0 , then τ is a shared nuisance parameter of that type. If the number of sources k is large we can safely profile, while if k is small we may need to resort to some of the corrections described next. Often we have both source-specific and shared nuisance parameters. In that case, we ideally need to have a large number of large sources in order to produce valid CDs with the default profiling-based method. Note that in these cases, if k is too small, large sources will not necessarily help. Conversely, if the n_j are too small, a large k will not in general be able to remedy the mistakes coming from profiling in the II step.

5.2 Corrections to the log-likelihood profile

There is a large literature concerning corrections or modifications to the profile likelihood. The different corrections appearing in the literature have varying performance and complexity; see for instance Barndorff-Nielsen (1986), Cox & Reid (1993), Diccio & Efron (1992), Stern (1997), DiCiccio et al. (1996). There is also a whole subfield of integrated likelihood methods with partly similar aims, see Berger, Liseo & Wolpert (1999). A thorough investigation of all these methods is outside the scope of this article, and we will therefore only present one rather simple, somewhat limited solution. Alternative methods might work better, or at least in a more general setting, but these are often more complicated to compute.

In Cox & Reid (1987), the authors present what we will term the simple Cox–Reid correction. This is possibly the easiest correction to compute among those suggested above. It can be considered a special case of the correction in the general modified profile likelihood of Barndorff-Nielsen, but the simple Cox–Reid correction is limited to situations with orthogonal parameters (i.e. that the off-diagonal terms in the expected information matrix are equal to zero). Assume we have a scalar parameter of interest ψ and some vector of nuisance parameters λ . As usual, the profile log-likelihood for ψ is defined as $\ell_{\text{prof}}(\psi) = \ell(\psi, \hat{\lambda}(\psi))$, where $\hat{\lambda}(\psi)$ is the ML estimate of λ for each fixed ψ value. The simple Cox–Reid correction gives the following modification of the profile log-likelihood,

$$\ell_{\text{cprof}}(\psi) = \ell_{\text{prof}}(\psi) - \frac{1}{2} \log[\det J_{\lambda\lambda}(\psi, \hat{\lambda}(\psi))] \quad (5.1)$$

where $J_{\lambda\lambda}(\psi, \hat{\lambda}(\psi)) = -\partial^2 \ell(\psi, \lambda) / (\partial \lambda \partial \lambda^t)$ is the observed information for the λ components, evaluated at $(\psi, \hat{\lambda}(\psi))$. The simple Cox–Reid correction can be used both in the II and FF steps, for models with orthogonal parameters. We illustrate the use of the Cox–Reid correction in the II step in the Appendix Section C. In the FF step, corrections may be necessary when there are shared nuisance parameters arising from a random effect distribution. In particular, we propose that this correction should readily be applied when the random effect distribution is assumed to be normal. Here, the correction should be particularly notable for small k . We will present some Cox–Reid corrections in a classic model for random effect meta-analysis in Section 6.

5.3 Optimal CD methods

For some parameters in exponential families, we can bypass the standard II-CC-FF, and its potential problems, by making use of the following alternative method which is much more powerful, producing *optimal CDs*. In our II-CC-FF setting, this method might come into play both in the II step and the FF step, see the application in Section 6.2.

For ease of presentation, we present the optimal confidence method in the case where all the k sources inform on a common focus parameter $\psi = \psi_1 = \dots = \psi_k$. This constitutes a situation where the method is used in the final FF step. Suppose again that ψ is the focus parameter, and that we have m nuisance parameters $\gamma_1, \dots, \gamma_m$, which may be both source-specific or shared across all k sources. Suppose also that the log-likelihood function at work, based on information sources y_1, \dots, y_k , can be written in the form

$$\ell(\psi, \gamma_1, \dots, \gamma_m) = \psi A + \gamma_1 B_1 + \dots + \gamma_m B_m - d(\psi, \gamma_1, \dots, \gamma_m) + h(y_1, \dots, y_k), \quad (5.2)$$

where A and B_1, \dots, B_m are statistics, i.e. functions of the data collection, with observed values A_{obs} and $B_{1,\text{obs}}, \dots, B_{m,\text{obs}}$, and with m often bigger than k . Then, under mild regularity conditions, there is an overall most powerful CD, namely

$$C^*(\psi, y) = P_{\psi} \{A \geq A_{\text{obs}} \mid B_1 = B_{1,\text{obs}}, \dots, B_m = B_{m,\text{obs}}\}.$$

That this $C^*(\psi, y)$ indeed depends on ψ but not on the γ_j parameters is part of the result and the construction.

To illuminate the exact meaning of ‘most powerful’ in this setting, one needs to consider the theory for loss and risk functions for CDs developed in Schweder & Hjort (2016, Ch. 5). Confidence power is measured via the risk function

$$r(C, \psi, \gamma) = E_{\psi, \gamma} \int \Gamma(\psi_{\text{cd}} - \psi) dC(\psi_{\text{cd}}, Y), \quad (5.3)$$

for any convex nonnegative $\Gamma(\cdot)$ with $\Gamma(0) = 0$. The random mechanism involved in the expectation here is a two-stage operation; first data y , governed by the (ψ, γ) held fixed, are used to generate the CD $C(\psi, y)$, and then ψ_{cd} is a random draw from this distribution. Intuitively, a low confidence risk means that the CD in question is tight around true value of ψ , while CDs which are less concentrated around the true value will have a higher risk. A CD with low confidence risk should therefore be expected to produce narrow confidence intervals (but keeping the correct coverage), and point estimates with little bias. We will see the confidence risk concept at work in Section 8.3.

6 Meta-analysis

As mentioned in the small start example (1.1), some common meta-analysis methods flow more or less directly from the II-CC-FF framework. In addition, the framework also invites more general, principled and non-standard solutions some which we will explore in this section. Further, we will investigate connections between II-CC-FF and a couple of widely encountered meta-analysis methods. We will start with a discussion of the basic random effect model, before we go on to the famous case of meta-analysis of 2×2 tables.

6.1 The basic random effect model

The most canonical type of random effect meta-analysis, which we term the basic random effect model, starts with k independent estimators y_1, \dots, y_k aiming at the parameters ψ_1, \dots, ψ_k , with $y_j | \psi_j \sim N(\psi_j, \sigma_j^2)$, and $\psi_j \sim N(\psi_0, \tau^2)$. Usually the source-specific standard deviations σ_j are assumed known. The literature treating this model is enormous, see for instance Langan et al. (2019) and Partlett & Riley (2017) and references therein. Note that likelihood-based method for the basic random effect model, even exploring higher order corrections, have been investigated earlier, see for instance Hardy & Thompson (1996) and Noma (2011). For a more general likelihood approach see O'Rourke (2008).

When assuming known σ_j , the integral in (4.2) has an explicit solution and the standard II-CC-FF solution will rely on the following log-likelihood function

$$\ell(\psi_0, \tau) = \sum_{j=1}^k \left\{ -\frac{1}{2} \log(\sigma_j^2 + \tau^2) - \frac{1}{2} \frac{(y_j - \psi_0)^2}{\sigma_j^2 + \tau^2} \right\},$$

where we profile out either ψ_0 or τ depending on which parameter is of main interest. The confidence curves for ψ_0 and τ will point at the standard ML estimators, and the ensuing confidence intervals will be very similar to solutions which have been investigated in some of the references mentioned above. These solution are reasonably good when k is not too small, see also Section 8.1, but may be improved upon. Langan et al. (2019) finds, for instance, that the ML estimator for τ has relatively poor performance in terms of bias and mean squared error.

We can attempt to improve on the standard II-CC-FF solution using the Cox–Reid correction. First we will consider the case where ψ_0 is the parameter of main interest, then the full combined profile likelihood from the FF step becomes

$$\begin{aligned} \ell_{\text{fus, cprof}}(\psi_0) = & \sum_{j=1}^k \left\{ -\frac{1}{2} \log(\sigma_j^2 + \hat{\tau}^2(\psi_0)) - \frac{1}{2} \frac{(y_j - \psi_0)^2}{\sigma_j^2 + \hat{\tau}^2(\psi_0)} \right\} \\ & - \frac{1}{2} \log \sum_{j=1}^k \left\{ -\frac{1}{2} \frac{1}{(\sigma_j^2 + \hat{\tau}^2(\psi_0))^2} + \frac{(y_j - \psi_0)^2}{(\sigma_j^2 + \hat{\tau}^2(\psi_0))^3} \right\}. \end{aligned} \quad (6.1)$$

The first part of the formula is the ordinary profile log-likelihood, the second part the simple Cox–Reid correction. We obtain the combined confidence curve using the Wilks approximation. This correction has been obtained by differentiating with respect to τ^2 in (5.1); note that a somewhat different correction term would have been obtained if we had differentiated with respect to τ . We have not seen this solution anywhere in the literature, and we investigate its performance in Section 8.1. In this situation τ is a ‘border parameter’, as the profiled ML estimate $\hat{\tau}(\psi_0)$ can be zero with positive probability. This happens precisely when

$$\sum_{j=1}^k \frac{1}{\sigma_j^2} \left\{ \frac{(y_j - \psi_0)^2}{\sigma_j^2} - 1 \right\} \leq 0, \quad (6.2)$$

and if this takes place there is an interval of such ψ_0 values. The correction term will then experience non-smoothness at the end points of that interval. To avoid this non-smoothness issue, where the rationale behind the Cox–Reid correction term does not easily apply, we set the entire correction term to zero when (6.2) takes place for some ψ_0 . The correction term should be especially important when there are few studies and the heterogeneity between them is large.

We can consider a variation of (6.1) in the case of the individual sources have few measurements, which means that the σ_j estimates become uncertain. The II-CC-FF can then provide more sophisticated solutions. In the II step, we have exact CDs for each ψ_j based on the Student’s t distribution, which we can convert to a confidence log-likelihood by exact conversion in the CC step. For the FF step, we use the general random effect method from (4.2), either with numerical integration or using the TMB package. Corrections in both the II and FF step may be considered, but we have not fully investigated these options yet.

Rather than focusing on the overall mean, as we did above, one may be interested in the overall spread τ . From the above, we have direct and Cox–Reid corrected log-likelihood profiles $\ell_{\text{fus,prof}}(\tau) = -\frac{1}{2}A_k(\tau)$ and $\ell_{\text{fus,cprof}}(\tau) = -\frac{1}{2}B_k(\tau)$, with

$$A_k(\tau) = \sum_{j=1}^k \left[\log(\sigma_j^2 + \tau^2) + \frac{\{y_j - \hat{\psi}_0(\tau)\}^2}{\sigma_j^2 + \tau^2} \right] \quad \text{and} \quad B_k(\tau) = A_k(\tau) + \log\left(\sum_{j=1}^k \frac{1}{\sigma_j^2 + \tau^2}\right),$$

with the profiled ML estimator $\hat{\psi}_0(\tau) = \sum_{j=1}^k \hat{\psi}_j / (\sigma_j^2 + \tau^2) / \sum_{j=1}^k 1 / (\sigma_j^2 + \tau^2)$ for each given τ . One might recognise the $-\frac{1}{2}B_k(\tau)$ as the log-likelihood associated with the so-called restricted ML or REML estimator for τ , see for instance Langan et al. (2019). The link between the Cox–Reid correction (and more general corrections) and the REML procedure has been known for some time, see Durban & Currie (2000) and also Cox & Reid (1987), but is possibly under-appreciated in the meta-analysis literature. The above leads to two deviance functions, using the direct and the corrected log-likelihood profiles,

$$D_{k,\text{ml}}(\tau) = A_k(\tau) - A_k(\hat{\tau}_{\text{ml}}) \quad \text{and} \quad D_{k,\text{cml}}(\tau) = B_k(\tau) - B_k(\hat{\tau}_{\text{cml}}),$$

with $\hat{\tau}_{\text{ml}}$ and $\hat{\tau}_{\text{cml}}$ the minimisers of $A_k(\tau)$ and $B_k(\tau)$. The distribution of $y_j - \hat{\psi}_0(\tau)$ does not depend on the underlying ψ_0 , which means that $D_{k,\text{ml}}(\tau)$ and $D_{k,\text{cml}}(\tau)$ have distributions only depending on the candidate value τ . Thus we have well-defined and exact confidence curves for τ ,

$$\text{cc}_{\text{ml}}(\tau) = P_{\tau}\{D_{k,\text{ml}}(\tau) \leq D_{k,\text{ml,obs}}(\tau)\} \quad \text{and} \quad \text{cc}_{\text{cml}}(\tau) = P_{\tau}\{D_{k,\text{cml}}(\tau) \leq D_{k,\text{cml,obs}}(\tau)\}. \quad (6.3)$$

We make use of these confidence curve methods in Application 9.1. The Wilks type chi-squared approximation works well for moderate to large values of k , but not for τ small, which often might

be the parameter region of primary interest, as for the application pointed to. Hence we need to compute the two confidence curves via simulations, with a high number of $D_{k,\text{ml}}(\tau)$ and $D_{k,\text{cml}}(\tau)$ generated for each candidate value τ .

In the normal-normal set-up above, the parameters are orthogonal, but we suggest that one could use the simple Cox–Reid correction even if the model for the observations in each source is non-normal. Suppose we are in a setting like in (4.2), and assume that the random effect distribution is normal, with the parameter of main interest being the overall mean ψ_0 . Inside each source we can have any (regular) model. In a simple normal model, the Cox–Reid correction when profiling out the variance τ^2 would be equal to $-\log\{\hat{\tau}(\psi)\}$. We propose to routinely use the following corrected likelihood profile construction in this type of random effect setting,

$$\ell_{\text{fus,cprof}}(\psi_0) = \sum_{j=1}^k \left\{ \log \left[\int \exp\{\ell_{\text{conv},j}(\psi_j)\} \frac{1}{\hat{\tau}(\psi_0)} \varphi \left(\frac{\psi_j - \psi_0}{\hat{\tau}(\psi_0)} \right) d\psi_j \right] \right\} + \log\{\hat{\tau}(\psi_0)\}, \quad (6.4)$$

where $\hat{\tau}(\psi_0)$ is the ML estimate of τ for each fixed ψ_0 value and φ is the standard normal density. The orthogonality of ψ_0 and τ in the full (integrated) distribution does not necessarily hold, but it would hold if the sources were large, since then $\ell_{\text{conv},j}(\psi_j)$ above will approach a normal likelihood. We therefore consider formula (6.4) to be an approximate correction for the situation when k is small, but the n_j are sufficiently large. In fact the correction term in (6.4) is a special case of the correction term in (6.1) when the σ_j go to zero (which of course corresponds to n_j increasing towards infinity). We investigate this idea in the situation of meta-analysis of 2×2 tables, see Section 8.2.

6.2 Meta-analyses of 2×2 tables

In meta-analyses of 2×2 tables, each study seeks to compare the probability of observing a certain binary event in the control group and in the treatment group. The counting variables $Y_{0,j}$ and $Y_{1,j}$ indicate how many patients have experienced the event in each group in study j . These variables are usually modelled as pairs of binomials, $Y_{0,j} \sim \text{binom}(m_{0,j}, p_{0,j})$ and $Y_{1,j} \sim \text{binom}(m_{1,j}, p_{1,j})$, with subscript ‘1’ indicating treatment and ‘0’ control, and the sample sizes in each group are denoted by $m_{0,j}$ and $m_{1,j}$. The most common measure for the treatment effect is the odds ratio, or equivalently, the log odds ratio ψ_j . For that effect measure it is convenient to express the event probabilities in the control and treatment groups as $p_{0,j} = \exp(\theta_j)/(1 + \exp(\theta_j))$, and $p_{1,j} = \exp(\theta_j + \psi_j)/(1 + \exp(\theta_j + \psi_j))$. Each study, or source, has a specific nuisance parameter θ_j , governing the event probability in the control group. We will first treat the fixed effect case where the log odds ratios are assumed common across all sources, $\psi_1 = \dots = \psi_k = \psi$, before we come to the random effect case in the next paragraph. The information available in each source depends on the binomial sample sizes $m_{0,j}$ and $m_{1,j}$, and on the event probabilities. If the number of studies increases while the size of each study stays constant, it is known that the ML estimator is inconsistent (Breslow, 1981), and we can expect that the standard II-CC-FF method will not work well. Also, the simple Cox–Reid correction to the profile in each source is not immediately available because ψ_j and θ_j are not orthogonal. However, there exists an optimal CD for the common ψ based on the theory from Section 5.3,

$$C_{\text{opt}}(\psi, \text{data}) = P_{\psi}(B_k > b \mid z_1, \dots, z_k) + \frac{1}{2} P_{\psi}(B_k = b \mid z_1, \dots, z_k). \quad (6.5)$$

Here, $z_j = y_{0,j} + y_{1,j}$ and $B_k = \sum_{j=1}^k Y_{1,j}$. The CD is obtained by simulating the distribution of B_k given Z_1, \dots, Z_k . The second part of (6.5) is a half-correction. Note also that we similarly

have an optimal CD for ψ_j within each source,

$$C_{\text{opt},j}(\psi_j, y_{0,j}, y_{1,j}) = P_\psi(Y_{1,j} > y_{1,j} | z_j) + \frac{1}{2}P_\psi(Y_{1,j} = y_{1,j} | z_j). \quad (6.6)$$

This CD is simple to compute as $Y_{1,j} | Z_j$ has an eccentric hypergeometric distribution. Note that this CD is very closely related to the method known as Fisher’s exact test (Fisher, 1954). Starting from (6.6) for each source in the II step, we can obtain an approximation to the optimal solution in (6.5) which is faster to compute and also lends itself to a natural random effect extension, as we will see. In the CC step, we use exact conversion to obtain the confidence log-likelihoods $\ell_{\text{conv},j}(\psi_j) = \log g_j(y_{1,j}, \psi_j)$, where

$$g_j(y_{1,j}, \psi_j) = \frac{\binom{m_{0,j}}{z_j - y_{1,j}} \binom{m_{1,j}}{y_{1,j}} \exp(\psi_j y_{1,j})}{\sum_{u=0}^{z_j} \binom{m_{0,j}}{z_j - u} \binom{m_{1,j}}{u} \exp(\psi u)} \quad \text{for } y_{1,j} = 0, 1, \dots, \min(z_j, m_{1,j}) \quad (6.7)$$

is the density function of the eccentric hypergeometric distribution. We sum these confidence log-likelihoods to get $\ell_{\text{fus}}(\psi) = \sum_{j=1}^k \ell_{\text{conv},j}(\psi_j)$, find the ML estimate $\hat{\psi}$ and the deviance, and use the Wilks approximation:

$$\text{cc}^*(\psi, \text{data}) = \Gamma_1(2\{\ell_{\text{fus}}(\hat{\psi}) - \ell_{\text{fus}}(\psi)\}). \quad (6.8)$$

Even though there is some level of approximation in this solution, it tends to work well, see Section 8.2.

From this approximate fixed effect approach we find a natural extension to random effects. Assuming that the log-odd ratios from the different sources come from a common normal distribution, we have the following fusion log-likelihood for the overall parameters,

$$\ell_{\text{fus}}(\psi, \tau) = \sum_{j=1}^k \log \left\{ \int g_j(y_{1,j}, \psi_j) \frac{1}{\tau} \varphi \left(\frac{\psi_j - \psi}{\tau} \right) d\psi_j \right\}, \quad (6.9)$$

where $g_j(y_{1,j}, \psi_j)$ is the density function of the eccentric hypergeometric distribution, pointed to above. If we are mainly interested in ψ_0 , we profile out τ and use the Wilks approximation. If the heterogeneity is big or the number of sources is small we add the approximate Cox–Reid correction $\log \hat{\tau}(\psi)$ from (6.4) to the profile log-likelihood. In applications, we computed the integral using the TMB package. This approach seems promising with good coverage properties in simulations (Section 8.2).

7 Other combination methods based on CDs

There is a steadily growing literature on combination of information with CDs. Here we will briefly discuss methods by Singh et al. (2005) and Liu et al. (2015). These CD approaches are sometimes collected under the same umbrella, called Fusion Learning (Cheng et al., 2017).

We start by discussing the approach of Singh et al. (2005), valid when all confidence components relate to a common focus parameter. Suppose that independent information sources y_1, \dots, y_k give rise to CDs for the same parameter, say $C_1(\psi, y_1), \dots, C_k(\psi, y_k)$. A general way of combining these into a single overall CD has been proposed and worked with by Singh et al. (2005), later on applied in various contexts by Xie et al. (2011), Xie & Singh (2013), Liu et al. (2014b), and others. The starting point is that under the true state of affairs, the $\Phi^{-1}(C_j(\psi, Y_j))$ are independent standard normals, from the basic properties of CDs; here $\Phi(\cdot)$ again denotes the

c.d.f. for the standard normal. Hence $\sum_{j=1}^k w_j \Phi^{-1}(C_j(\psi, Y_j))$ is also standard normal, when the weights w_j are such that $\sum_{j=1}^k w_j^2 = 1$. This again implies that

$$\bar{C}(\psi, y) = \Phi\left(\sum_{j=1}^k w_j \Phi^{-1}(C_j(\psi, y_j))\right) \quad (7.1)$$

is a CD for ψ , using the combined dataset $y = (y_1, \dots, y_k)$. The idea generalises to other basic distributions than the normal, but then the required convolutions become less tractable.

For the prototype situation associated with (1.1), the individual CDs take the form $C_j(\psi, y_j) = \Phi((\psi - y_j)/\sigma_j)$, and the general (7.1) recipe yields

$$\bar{C}(\psi, y) = \Phi\left(\sum_{j=1}^k w_j (\psi - y_j)/\sigma_j\right).$$

Some considerations then lead to the best of these linear combinations, with weights w_j proportional to $1/\sigma_j$ and $\sum_{j=1}^k w_j^2 = 1$. This indeed agrees with the standard method (7.1).

Recipe (7.1) requires nonrandom weights w_j , and these could in various cases be fruitfully taken as proportional to $1/\sqrt{m_j}$, with m_j the sample size associated with data source y_j . In many other situations the balance is more delicate, however, perhaps demanding nonrandom weights, of the type \hat{w}_j estimating an underlying optimal but not observable $w_{j,0}$. Problems worked with in Liu et al. (2014b) are of this type. In such cases recipe (7.1) is not entirely appropriate and is rather to be seen as an approximation, associated with confidence intervals with approximate levels of confidence.

The approach described above yields approximative solutions for the basic normal-normal random effect model, partly helped by the fact that the unconditional density in that case has an explicit normal form, $y_j \sim N(\psi_0, \sigma_j^2 + \tau^2)$. It is not clear how the method in Xie et al. (2011) can incorporate more general random effect models, however.

Under the ‘Fusion learning’ umbrella there are other methods. The method in Liu et al. (2015) may be termed a ‘confidence density method’ and can be considered as a special case of II-CC-FF, as we will see. The method is proposed for a fixed effect setting, but where the studies may differ in reported outcomes, in measured covariates, or have source-specific nuisance parameters. Thus, some of the studies may only contain indirect information about the parameter of interest. Let θ be the full parameter vector for all the studies and $\gamma_j = M_j(\theta)$ the parameters in study j , with M_j denoting a known mapping function. Liu et al. (2015) summarise the information in each source with multivariate normal CDs, $C_j(\gamma_j, y_j)$, transform these to confidence densities $c_j(\gamma_j, y_j) = \partial C_j(\gamma_j, y_j)/\partial \gamma_j$, which are then multiplied into a combined confidence density, which informs on the full θ . The authors stress that the approach is general in the sense that it can be used with a wide range of parametric models for the sources. This generality is achieved because the authors assume that the number of observations in each source increases to infinity.

The normal CDs for each study only requires the estimated parameter vector $\hat{\gamma}_j$ and estimated covariance matrix $\hat{\Sigma}_j$ for $\hat{\gamma}_j$, and the authors therefore highlight that the approach only needs summary statistics rather than the full data. Also, they prove that their approach is asymptotically equally efficient as a traditional likelihood approach using the full data.

For location parameters in normal models the confidence density and confidence likelihood are proportional. The approach in Liu et al. (2015) can therefore be considered a special case of II-CC-FF. Sometimes the confidence density might be easier to obtain than the exact confidence

log-likelihood, and could be used also in connection with II-CC-FF. However, one might need to be careful, as this approach could introduce mistakes. The confidence density is equal to $\partial C(\psi, T)/\partial \psi$, while the exact confidence likelihood takes the derivative with respect to T , as we saw in Section 3. The difference between the confidence density and confidence likelihood will be the most pronounced when the sample sizes are small, with the difference going away with increasing sample sizes.

8 Performance evaluations

The main benefit of our II-CC-FF framework is its general nature and wide applicability, and in the next section we will therefore demonstrate the use of II-CC-FF in several non-standard combination situations. Still, we also require that methods coming out of II-CC-FF should be competitive against other methods from the literature when applied to typical combination situations, for example meta-analysis settings. Here we will study the performance of II-CC-FF methods in two very classical situations: first in the basic random effect model and then in the meta-analysis of 2×2 tables. Both of these types of meta-analyses were discussed in Section 6, along with some notation which will be used in this section too. Finally, in the last subsection we will study confidence risk functions for some II-CC-FF schemes, compared to other CD combination methods, in a particular simplified example.

8.1 The basic random effect model

We have investigated some of the methods from Section 6.1 with a simulation study inspired by Langan et al. (2019). We treat the setting where ψ_0 is the parameter of main interest. In that setting Langan et al. (2019) found that confidence intervals computed by the Hartung-Knapp-Sidik-Jonkman method were the clear winners in terms of coverage properties. That method uses the traditional inverse-variance method for the point estimator, and computes confidence intervals based on the t-distribution and the following variance formula,

$$\text{Var}_{\text{HKSJ}} \hat{\psi}_0 = \frac{\sum_{j=1}^k (\hat{\psi}_j - \hat{\psi}_0)^2 / (\hat{\sigma}_j^2 + \hat{\tau}^2)}{(k-1) \sum_{j=1}^k 1 / (\hat{\sigma}_j^2 + \hat{\tau}^2)}.$$

This formula requires one to plug-in an estimator for τ and for this we used the REML estimator, as recommended by Langan et al. (2019). We will compare this state-of-the-art method with our standard II-CC-FF method, and the II-CC-FF method using the corrected log-likelihood profile in (6.1). We will also include the method for the basic random effect model which comes out of the CD combination framework of Xie et al. (2011). This method is implemented in the `gmeta` package (Yang et al., 2016). See Appendix A for more details.

We let $\psi_0 = 0.5$ and consider two values for the between-study heterogeneity, $\tau = 0.09$ for a scenario with little heterogeneity and $\tau = 0.44$ for a scenario with large heterogeneity. Further, we choose $\sigma_j = 2/\sqrt{m_j}$ with $m_j \sim \text{unif}(30, 50)$, and investigate four values for the number of studies, 5, 10, 20, 50. We generated 10000 meta-analyses for each k value. For a single meta-analysis, ψ_j and σ_j were estimated using their ordinary estimators in each of the k studies (even though all the methods assume that the σ_j are known). For each method, we recorded the coverage rate of 95% confidence intervals, the width of these intervals, and point estimates for ψ_0 .

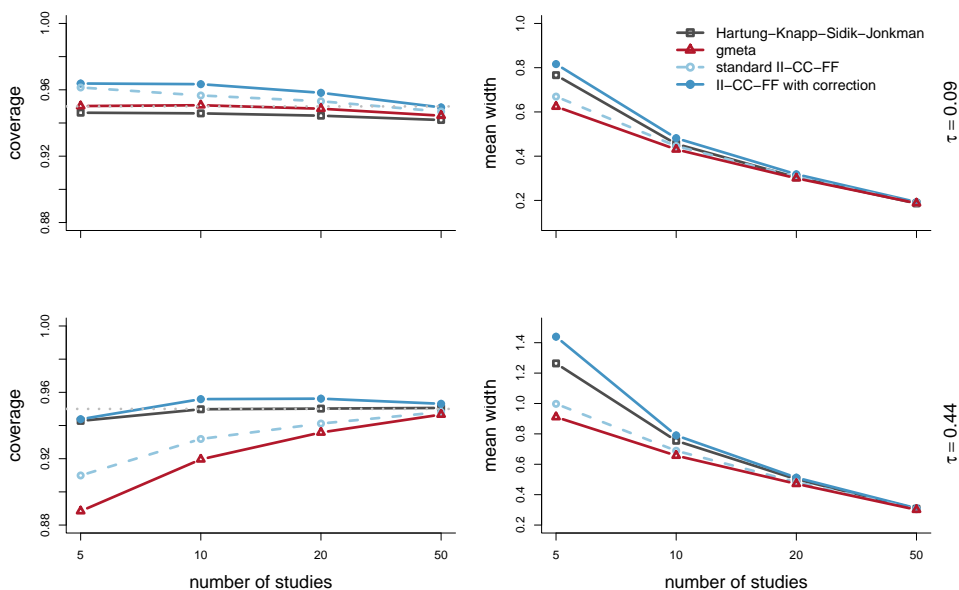


Figure 8.1: Simulation results for the basic random effect model. The left plot gives the realised coverage rate of 95% confidence intervals, the right plot gives the median width of these intervals. The results in the top row are for a scenario with small between-study heterogeneity, while in the bottom row the between-study heterogeneity is large.

The confidence intervals from the Hartung-Knapp-Sidik-Jonkman method have perfect coverage rate for almost all k values in both scenarios (Figure 8.1), which is consistent with results in Langan et al. (2019). The CD method from Xie et al. (2011) has very good performance in the scenario with small heterogeneity, but severe under-coverage in the scenario with large heterogeneity. The standard II-CC-FF method has a similar problem in that scenario, but the II-CC-FF version with corrected profile likelihood obtains coverage rates close to the nominal 0.95. Both II-CC-FF versions are slightly conservative in the small heterogeneity scenario, but obtain nonetheless confidence intervals of similar mean width as the Hartung-Knapp-Sidik-Jonkman intervals. The four methods produce virtually identical point estimates for ψ_0 . All in all we find the II-CC-FF method to have almost equally good performance as the state-of-the-art method. In scenarios with low heterogeneity the correction to the profile likelihood is not important, while it is crucial in scenarios with large between-study heterogeneity.

8.2 Meta-analyses of 2×2 tables

We will investigate both the fixed effect and random effect cases. Our simulation set-ups are inspired by two recent papers with extensive simulation studies: Piaget-Rossel & Taffé (2019) for the fixed effect case and Jackson et al. (2018) for the random effects case. With fixed effects, we will investigate three common effect measures: the (log) odds ratio defined in Section 6, the (log) risk ratio, $\exp(\psi_j) = p_{1,j}/p_{0,j}$, and the risk difference, $\psi_j = p_{1,j} - p_{0,j}$. With random effects, we will only treat the odds ratio, however.

Piaget-Rossel & Taffé (2019) focus on meta-analyses with rare events, i.e. where both the treatment and control group have low event probabilities and where there may be many studies with zero events. The overall conclusion of the paper was that the Mantel-Haenszel method had the best performance among the methods that were considered. This method is applicable to all

three effect measures mentioned above, and Piaget-Rossel & Taffé (2019) found that it produced confidence intervals with good coverage properties, and point estimates with relatively small bias. The Mantel-Haenszel is a well-established method, which was originally proposed in 1959 (Mantel & Haenszel (1959) and extended in Rothman et al. (2008)). The method offers explicit estimators for the log odds ratio, log risk ratio and risk difference, as well as expressions for the variance of these estimators. Confidence intervals are computed using the Wald approximation. We will compare some variants of our II-CC-FF scheme with the Mantel-Haenszel method. We will also include methods reviewed in Liu et al. (2014a). These methods are based on exact tests and fall into the unifying CD framework of Singh et al. (2005) which we described in Section 7. For the odds ratio and risk difference, these CD methods have been implemented in the `gmeta` package (Yang et al., 2016); for the risk ratio a related exact method is implemented in the `exactmeta` package (Yu & Tian, 2014). See Appendix A for more details.

For all three effect measures we will make use of the standard II-CC-FF procedure which consists of profiling out the nuisance parameters in each source, summing the log-likelihood profiles, and then using the Wilks approximation to obtain a confidence curve for ψ , from which we can extract confidence intervals and point estimates. For the odds ratio case we will include two additional variants that can be said to fall under the II-CC-FF umbrella: the optimal CD method given in (6.5) and the II-CC-FF method using exact conversion, which we give in (6.8). This II-CC-FF version resembles the standard II-CC-FF procedure, but avoids the profiling step by making use of the conditional log-likelihood for ψ_j , in (6.7).

We simulated datasets with a median event probability of 0.005 in the control group. According to the simulation study in Piaget-Rossel & Taffé (2019) we can expect that this will be a challenging setting for all methods we consider. We generated baseline probabilities $p_{0,j} = \exp(\theta_j) / \{1 + \exp(\theta_j)\}$ by drawing $\theta_j \sim N(\log \frac{0.005}{1-0.005}, 0.5)$, $m_{1,j} \sim \text{unif}(50, 150)$ and $m_{0,j} = r_j m_{1,j}$ with $r_j \sim \text{unif}(0.5, 1.5)$ (so we have some variation in which of the groups has the most participants). The probabilities in the treatment group were computed according to the chosen effect measure,

$$\begin{aligned} \text{Odds ratio:} \quad & p_{1,j} = \frac{\exp(\theta_j + \psi)}{1 + \exp(\theta_j + \psi)} \quad \text{with the log odds ratio } \psi = -1.5, \\ \text{Risk ratio:} \quad & p_{1,j} = \exp(\psi)p_{0,j} \quad \text{with the log risk ratio } \psi = -1.5, \\ \text{Risk difference:} \quad & p_{1,j} = \psi + p_{0,j} \quad \text{with the risk difference } \psi = 0.05. \end{aligned}$$

We let k , the number of studies, take the values 5, 10, 20 and 50. For each set-up we generated 10000 meta-analyses, except in the risk difference set-up where we only generated 1000 (because the `gmeta` package was extremely slow for this effect measure). For each method we computed the coverage rate of 95% confidence intervals, the median width of these intervals, and the median bias of the point estimates coming out of the methods. Both the odds ratio and risk ratio were analysed on the log scale.

Results are presented in Figure 8.2. When there are few studies, most methods struggle with over-coverage in the odds ratio and risk ratio set-ups, but the Mantel-Haenszel method and the various II-CC-FF schemes come close to the nominal level as k increases. For the odds ratio, the standard II-CC-FF and the II-CC-FF with exact conversion have practically identical performance: both have some degree of under-coverage for $k = 20$, but come very close to the nominal 0.95 for $k = 50$. This seems to indicate that even though we are in a rare events setting, there is nonetheless sufficient information within each source so as to safely profile out the θ_j . The under-coverage experienced by these methods for $k = 20$ indicates that the Wilks approximation is not perfectly

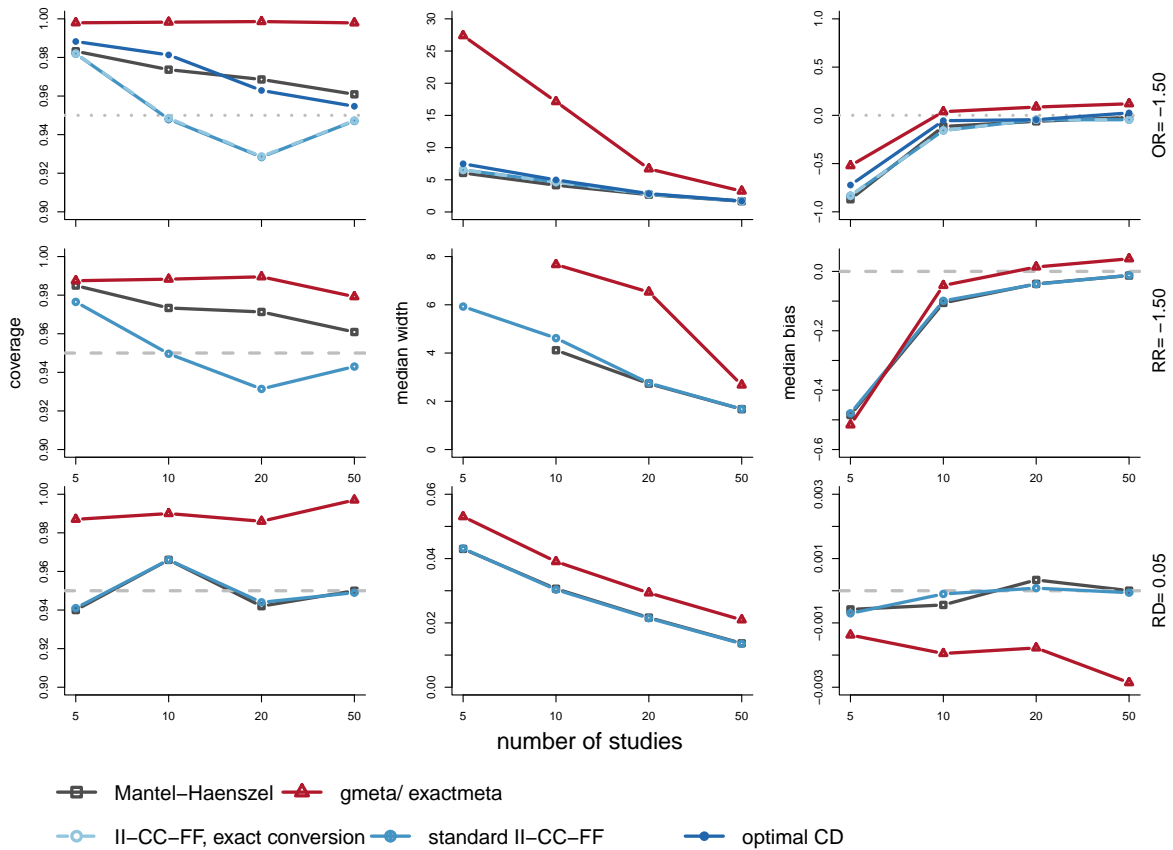


Figure 8.2: Simulation results for fixed effect meta-analysis of 2×2 tables. The left column gives the realised coverage rate of 95% confidence intervals, the middle column gives the median width of these intervals and the right column gives the median bias of the point estimate coming from each of the methods. The top row gives the results for the (log) odds ratio, the middle row for the (log) risk ratio and the bottom row gives the results for the risk difference. When k is small the confidence intervals can sometimes have infinite width (which explains the missing points for the log risk ratio).

fine, and one could consider adjustments, like for instance the Bartlett correction. The standard II-CC-FF has reasonably good coverage properties for the risk ratio and risk difference. For the risk ratio there is again some degree of under-coverage for $k = 20$, but for the risk difference there is no such pattern. In that setting, the Mantel-Haenszel method and the standard II-CC-FF method have practically identical performance. The `gmeta` and `exactmeta` methods are very conservative in all these experiments and consistently produce very wide 95% intervals, with a coverage rate close to 1. When there are few events, all methods tend to underestimate the effect measure (giving a negative median bias). As k increases all methods come closer to the true effect, except for the `gmeta` method for the risk difference which appears to get worse. For the odds ratio and risk ratio however, the `gmeta` method produces point estimates with somewhat smaller median bias than the other methods for some values of k .

Overall, II-CC-FF performs similarly, and at best, slightly better than the main existing competitor (according to Piaget-Rossel & Taffé (2019)). The II-CC-FF and the Mantel-Haenszel methods have generally similarly wide confidence intervals, but II-CC-FF intervals have a coverage rate often coming closer to the nominal level. Sometimes the standard II-CC-FF method produces intervals with some degree of under-coverage, but the optimal CD method (which is only available

for the odds ratio) does not. The methods reviewed in Liu et al. (2014a) perform very poorly in the settings we have presented here. We have included a simulation study with less extreme event probabilities in the appendix. There the median event probability in the control group is 0.1. That situation is less challenging for all the methods, and most obtain a coverage rate close to 0.95 even for small k . The `gmeta` method has acceptable performance in that setting, at least for the odds ratio. For the risk difference the results are still quite poor.

Some readers might be puzzled by the fact that the optimal CD method for the odds ratio does not have even better performance in the simulations. This CD is optimal in the sense of Section 5.3 and one might think that it should have exact coverage properties. For discrete data as we have here, the method of Section 5.3 requires a half-correction, as we see in (6.5). In settings with few tables and few events, the statistics encountered will attain only few possible values, and so have particularly non-continuous distributions; this likely explains the results we see in these simulations.

Finally, note that in rare events settings it might be fruitful to assume that the event counts in the two groups are Poisson distributed rather than binomials, see for instance Cai et al. (2010) and Cunen & Hjort (2015). Our II-CC-FF framework can naturally be applied to such models too and would produce different results than the ones we see here.

In Jackson et al. (2018) the authors compare seven methods for odds ratio meta-analysis of 2×2 tables in a random effects setting. Many authors find random effects methods, and implicitly random effects models, to be preferable to fixed effects methods for this type of meta-analysis, since it may seem more realistic to allow for some heterogeneity in the treatment effects between the studies. As is commonly done, we will assume that the log odds ratios come from a normal distribution, $\psi_j \sim N(\psi_0, \tau^2)$. In their simulation study, Jackson et al. (2018) found that several of the methods had similar (equally good) performance. Among others, they recommend the use of a modified version of the Simmonds & Higgins (2016) method, for its ease of use and good performance. The method uses a generalised linear mixed effect framework to estimate ψ_0 and τ (and the θ_j) by assuming that the logit of $(p_{0,j}, p_{1,j})$ are drawn from a bivariate normal distribution with expectation $(\theta_j, \theta_j + \psi_0)$ and a certain covariance matrix (with variances equal to $\tau^2/4$). The modified Simmonds-Higgins method is implemented in the `metafor` package (Viechtbauer, 2010), and we will compare our II-CC-FF methods with this. The other CD methods we reviewed in Section 7 do not provide a readily applicable method for these type of random effects situations.

We will investigate two II-CC-FF versions here. The first version constitutes the standard II-CC-FF solution for random effects. We use (6.9), profile out τ and use the Wilks approximation to obtain the combined confidence curve for ψ_0 . The second version makes use of the same profile log-likelihood, but adds the approximate Cox–Reid correction as suggested in the text under (6.9). The idea is that this correction will account for the error from having profiled out τ . We compute the integral in (6.9) using the `TMB` package. Note that we do not compute the correction in rounds where τ is estimated to be very close to zero (below 0.0001), since in that case the correction blows up.

Jackson et al. (2018) include many different scenarios in their simulations, but we limit ourselves to one main scenario, where we let the number of studies, k , vary as we did in the previous subsection. We use $\theta_j \sim N(\log \frac{0.2}{1-0.2}, 0.3^2)$ giving median baseline probabilities of 0.2, $m_{1,j} \sim \text{unif}(10, 50)$ and $m_{0,j} = m_{1,j}$. Further, we let $\psi_j \sim N(0, 0.168)$, which gives considerable heterogeneity in the treatment effects. We generated 10000 meta-analyses for each value of k

(5, 10, 20 and 50).

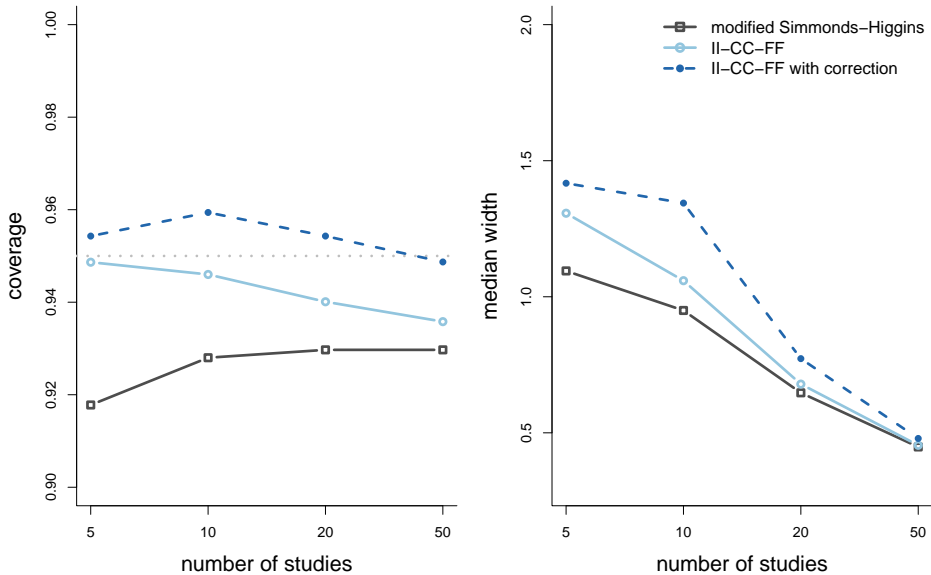


Figure 8.3: Simulation results for random effect meta-analysis of 2×2 tables. The left plot gives the realised coverage rate of 95% confidence intervals, the right plot gives the median width of these intervals.

For each method we computed the coverage rate of 95% confidence intervals, the median width of these intervals, and we recorded the point estimates coming out of the methods. In Figure 8.3 we display the coverage rate and median width results. Both the modified Simmonds and Higgins and standard II-CC-FF methods produce confidence intervals with some degree of under-coverage. For the modified Simmonds and Higgins method this is consistent with the results in Jackson et al. (2018) for scenarios with considerable heterogeneity in the treatment effects and small within-study sample sizes (as we have here). Surprisingly, the coverage rate of the intervals from the standard II-CC-FF seems to worsen as k increases. The performance of the corrected II-CC-FF method in terms of coverage rate is very good. The effect of the correction seems substantial even when k is quite large. This is somewhat unexpected, but probably due to the relatively large τ value in this scenario. For $k = 50$, the median widths of confidence intervals from the three methods are almost identical. If we had displayed the mean widths instead, we would have seen that the corrected II-CC-FF method in fact has larger *mean* width, which explains the higher coverage rate. Note that the Cox-Reid correction term in this case usually only widens the confidence curve, and only rarely shifts the point estimates.

The three methods produce very similar estimates of ψ_0 and τ . The bias for ψ_0 is small, but all three methods tend to under-estimate τ , which is a feature they share with all the methods investigated in Jackson et al. (2018). Remember that the II-CC-FF methods are in this case focussing on ψ_0 , and if τ had been of primary interest we would have used the confidence curve given in (6.3).

In Appendix A we include a similar figure for a scenario with less heterogeneity and higher within-study sample sizes. In that case, the modified Simmonds-Higgins method has close to correct coverage rate for all values of k , while both II-CC-FF methods are slightly conservative. When τ is small the correction term seldom changes the confidence curve, and the two II-CC-FF confidence curves are therefore often very similar in that scenario.

Again, we find II-CC-FF to have an overall good performance. In situations with large heterogeneity the corrected II-CC-FF method outperforms the recommended method from the literature. The scenarios we have investigated here have quite large event probabilities, and it is conceivable that the results would be somewhat different in a rare events setting. We hope to investigate this issue further in a separate paper.

Our standard II-CC-FF solution has actually been suggested previously, in Stijnen et al. (2010), and also in Van Houwelingen et al. (1993), as the hypergeometric-normal model. This model is in fact among the seven studied in Jackson et al. (2018), and while it obtains reasonably good performance in their simulations, the authors report numerical problems and estimation failure. This could be related to a different implementation than ours and particularly to the Laplace approximations used in the TMB package. We did not find that the standard II-CC-FF had a high probability of failure in the scenarios we investigated, but we readily acknowledge that further implementation efforts are necessary in order to make the method widely applicable. The approximate Cox-Reid correction which we found fruitful in settings where the standard II-CC-FF tended to produce anti-conservative intervals was not investigated in Jackson et al. (2018), or anywhere else in the literature as far as we know.

8.3 Confidence risk in a prototype example

To see how versions of the II-CC-FF scheme fare against natural competitors, in terms of leading to accurate CDs for focus parameters, consider the following simple setup. Independent gamma distributed variables $Y_j \sim \text{Gam}(a_j, \theta)$ are observed for $j = 1, \dots, k$, with densities proportional to $y_j^{a_j-1} \exp(-\theta y_j)$, with known shape parameters a_j and unknown scale parameter θ . Insights gleaned from studying performance in such a prototype setup should be helpful when analysing more complex situations. Here the canonical CD for data source y_j alone is

$$C_j(\theta, y_j) = P_\theta\{Y_j \leq y_j\} = G(\theta y_j, a_j, 1),$$

with $G(\cdot, a_j, 1)$ the c.d.f. of the $\text{Gam}(a_j, 1)$ distribution. The II-CC-FF scheme, using the directly available log-likelihood components, leads here to

$$\ell_{\text{fus}}(\theta) = \sum_{j=1}^k (a_j \log \theta - \theta y_j) = a. \log \theta - \theta y.,$$

writing $a. = \sum_{j=1}^k a_j$ and $y. = \sum_{j=1}^k y_j$. From $y. \sim \text{Gam}(a., \theta)$, its natural associated CD is $C^*(\theta, y) = G(\theta y., a.)$. By the optimality theorem of Section 5.3, this CD uniformly outperforms all competitors, in terms of all risk functions of the (5.3) type.

Competitors to consider, for performance comparisons, include the following. (i) The CD method of Singh et al. (2005), with the normal transformation, as in (7.1), with $C_j(\theta_j, y_j)$ as above, and with the natural choice $w_j = (a_j/a.)^{1/2}$. (ii) The ML estimator is $\hat{\theta} = a./y.$, and CDs may be constructed based on its exact or approximate distribution. The deviance function associated with the log-likelihood function is found to be

$$D_{\text{fus}}(\theta) = 2\{\ell(\hat{\theta}) - \ell(\theta)\} = 2\{a. \log(\hat{\theta}/\theta) - (\hat{\theta} - \theta)y.\} = 2a. \{\log(\hat{\theta}/\theta) - (\hat{\theta} - \theta)/\hat{\theta}\}.$$

Its distribution is independent of θ . Indeed, from $y. \sim \text{Gam}(a., \theta)$ one may write $\hat{\theta} \sim \theta/V$, in terms of $V \sim \text{Gam}(a., 1)/a.$, and from this follows the representation $D = 2a.(V - 1 - \log V)$. An exact

confidence curve is therefore

$$cc_{\text{fus}}(\theta, y) = H(D_{\text{fus}}(\theta), a.),$$

writing $H(x, a.)$ for the c.d.f. of the D . For moderate to large $a.$, some analysis shows $D \doteq a.(V - 1)^2$, and in particular $H(x, a.)$ is then close to the chi-squared distribution $\Gamma_1(x)$, in line with the Wilks theorem. Inspection shows that the χ_1^2 approximation works well already from say $a. \geq 6.0$, so only for smaller values is it worthwhile computing the exact $H(D_{\text{fus}}(\theta), a.)$. The $a.$ factor needs to be bigger in order for the normal approximation based $\Phi(a.^{1/2}(1 - \theta/\hat{\theta}))$ to come close to the $\Gamma_1(D_{\text{fus}}(\theta))$, however. (iii) We also point to the ‘confidence density method’ argued for in Liu et al. (2015), in essence consisting in deriving the confidence densities from the individual CDs, here taking the form $c_j(\theta) = g(\theta y_j, a_j, 1)y_j$, and then treating the resulting $c_1(\theta) \cdots c_k(\theta)$ as a likelihood function. In the present case, this is seen to be proportional to $\theta^{\sum_{j=1}^k (a_j - 1)} \exp(-\theta y.)$, leading to the estimator $\tilde{\theta} = (a. - k)/y.$, which has a sometimes severe negative bias. This serves to note that approximate CDs coming from the general recipes associated with combination of confidence densities may not work well, without further fine-tuning. It does work well in the multinormal setups studied in Liu et al. (2015), where confidence densities become identical to the converted log-likelihoods, but not in general.

We may illustrate the general performance theory by using $\Gamma(u) = |u|$ in (5.3), so risk is measured by the smallness of $E_\theta |\theta_{\text{cd}} - \theta|$. Again θ_{cd} is a random draw from the CD in question, which is itself the result of random data. For the best method $C^*(\theta, y)$, some analysis shows that $r^*(\theta) = r_0\theta$, with $r_0 = E |G_1/G_2 - 1|$, where G_1 and G_2 are independent draws from the $\text{Gam}(a., 1)$ distribution. The methods based on the $\ell_{\text{fus}}(\theta)$, as both this optimal $C^*(\theta, y)$ and those using the deviance, offer sometimes drastic improvements over both the Liu et al. (2014b, 2015) methods. for either small or big θ , depending on both k and the sizes of the a_j . The improvement is most noticeable in cases with many groups and small a_j . There is no simple expression for the risk $r(\theta)$ for the Singh et al. (2005) method, but it may be computed numerically by simulating for each value of θ a high number of $|\theta_{\text{cd}} - \theta|$ in the natural two-stage fashion; first data y from the model, leading to the CD $C(\theta, y)$, then θ_{cd} from this distribution.

9 Applications

Below we illustrate the capacity for the II-CC-FF paradigm to solve problems in four rather different application settings. The first application concerns an interesting archaeological dataset. Here we use the so-called basic random effect model which was discussed in Sections 6.1 and 8.1, but perhaps atypically our parameter of main interest is the spread parameter, not the overall centre parameter. For this spread parameter we construct exact CD methods for the FF step. The annual growth rate of humpback whales is the focus of our second application story. There we illustrate how to construct confidence curves based on non-sufficient summary statistics; we only have access to a point estimate and a highly non-symmetric confidence interval. In this example we also demonstrate how partial prior information can be incorporated into our II-CC-FF framework. Our third story concerns the development over time of the median Body Mass Index for Olympic speekskaters, where part of the the challenge is to construct and then convert accurate nonparametric CDs for sample medians to parametric log-likelihood terms. Finally, the last application illustrates the combination of ‘hard’ with ‘soft’ data. Here ‘hard’ designates data

sources of high quality which inform directly on the focus parameter. ‘Soft’ data, on the other hand, may be of lower quality, with more noise and biases, or simply containing less direct information on the focus parameter. Such large, noisy datasets are increasingly available in a number of fields, for example from webscraping or text-mining, but lead to challenges when attempting to fuse the sources. We illustrate the combination of ‘hard’ and ‘soft’ data with a grand question from the field of peace and conflict research; is there evidence for The long peace, and in that case, when did it start?

9.1 Skullometrics

In their fascinating anthropometrical study of the inhabitants of Upper Egypt, from the earliest prehistoric times to the Mohammedan Conquest, Thomson & Randall-Maciver (1905) report on skull measurements for more than a thousand crania. A subset of their data is reported on and analysed in Claeskens & Hjort (2008, Chs. 1 and 9), see in particular their Figures 1.1 and 9.1. This pertains to four cranium measurements, say $y = (y_1, y_2, y_3, y_4)^t$, for 30 skulls, from each of five Egyptian time epochs, corresponding to $-4000, -3300, -1850, -200, 150$ on our A.D. scale. We model these vectors as

$$Y_{j,i} \sim N_4(\xi_j, \Sigma_j) \quad \text{for } i = 1, \dots, 30,$$

for each of the five epochs j . There is a variety of parameters worth recording and analysing, where the emphasis is on identifying the necessarily small changes over time, related to the history of emigration and immigration in ancient Egypt; see also Schweder & Hjort (2016, Example 3.10). For the present illustration we choose to focus on the variance matrices, not the means, and consider

$$\psi = \{\max \text{eigen}(\Sigma)\}^{1/2} / \{\min \text{eigen}(\Sigma)\}^{1/2},$$

the ratio of the largest root-eigenvalue to the smallest root-eigenvalue of the variance matrix of the four skull measurements. This is the ratio of the largest to the smallest standard deviations of linear combinations $a^t Y$ of the four skull measurements, normalised to have coefficient vector length $\|a\| = 1$. This parameter is one of several natural measures of the degree to which the skull distribution is ‘stretched’. The question is whether the stretch parameter ψ has changed over time. We assess the degree of change, if any, via the spread parameter τ in the natural model taking $\psi_1, \dots, \psi_5 \sim N(\psi_0, \tau^2)$. Rather than merely providing a test of the implied hypothesis $H_0: \psi_1 = \dots = \psi_5$, which is equivalent to $\tau = 0$, with its inevitable p-value and a yes-no answer as with a traditional one-way layout type test, we aim at giving a full CD for τ , again applying the II-CC-FF scheme.

Table 9.1 gives point estimates

$$\hat{\psi}_j = \{\max \text{eigen}(\hat{\Sigma}_j)\}^{1/2} / \{\min \text{eigen}(\hat{\Sigma}_j)\}^{1/2}$$

for the five time epochs, along with estimated standard deviations σ_j for these estimators, the latter obtained via parametric bootstrapping from the estimated multinormal distributions. For our present purposes the underlying distributions for the estimators are approximately normal, with the standard deviations σ_j approximately known. Figure 9.1 displays point estimates with 0.90 confidence intervals (left panel), for the five epochs.

Using log-likelihood fusion methods derived in Section 6.1, involving profiling and corrections, we may compute the confidence curves $cc_{\text{ml}}(\tau)$ and $cc_{\text{cml}}(\tau)$, as per (6.3). These involve simulation

Table 9.1: Skulls: For each of the five time epochs, the table gives the estimate $\widehat{\psi}$ and its estimated standard deviation $\widehat{\sigma}$. See Section 9.1 and Figure 9.1.

epoch	$\widehat{\psi}$	$\widehat{\sigma}$
-4000	2.652	0.561
-3300	2.117	0.444
-1850	1.564	0.331
-200	2.914	0.620
150	1.764	0.373

of a high number of deviance statistics for each candidate value of τ . The resulting confidence curves are shown in Figure 9.1 (right panel). The direct profile method can be shown to have a clear negative bias, particularly so for smaller values of k . For the present case of $k = 5$ the corrected version $cc_{\text{cml}}(\tau)$, with median confidence estimate 0.272, is better than the direct version $cc_{\text{ml}}(\tau)$, with median confidence estimate 0.006. A third and simpler to compute CD for τ is via

$$Q_k(\tau) = \sum_{j=1}^k \frac{\{\widehat{\psi}_j - \widehat{\psi}_0(\tau)\}^2}{\sigma_j^2 + \tau^2} \quad \text{and} \quad C(\tau, \text{data}) = 1 - \Gamma_{k-1}(Q_{k,\text{obs}}(\tau)),$$

the point being that $Q_k(\tau)$ for a given true value of τ has the χ_{k-1}^2 distribution; see Schweder & Hjort (2016, Ch. 13). We note that these confidence curves have point masses at zero, hence also the associated CDs, via $cc(\tau) = |1 - 2C(\tau)|$. For each, the $C(0)$ has a clear interpretation as the p-value for testing $\tau = 0$ against $\tau > 0$. For the corrected profile CD, we find $C(0) = 0.123$, not small enough to warrant a claim that this particular ψ parameter has changed over the four thousand years of Egyptian history – other skullometric parameters have however changed; see Claeskens & Hjort (2008, Section 9.1) and Schweder & Hjort (2016, Example 3.5). An accurate 0.90 interval for τ , using the corrected profile, also indicated in the figure, is $[0, 1.085]$, with median confidence estimate is 0.272.

In other applications of this type of extended meta-analysis machinery the centre value ψ_0 of the background distribution of the ψ_j might be of high importance. For the skulls analysis the primary question is whether the ψ_j parameter, or other similar parameters associated with the Σ_j matrices, have changed over the course of four thousand years, and the precise value of ψ_0 is of secondary importance. We report, though, that the corrected log-profile methods of Section 6.1, see (6.1), lead to overall point estimate 1.980, with an accurate 90% interval stretching from 1.662 to 2.480. These intervals are not symmetric around the point estimate; see left panel of Figure 9.1.

9.2 Abundance of humpback whales

The II-CC-FF paradigm readily lends itself to combination of information from published sources, where we may not have access to the full data, but only summary measures. Paxton et al. (2009) provide estimates of the abundance of humpback whales in the North Atlantic in the years 1995 and 2001. The two estimates are based on different surveys and can be considered independent. The authors also provide 95% confidence intervals, via a somewhat complicated model involving aggregation of line transect data from different areas via spatial smoothing, and also includes bootstrapping. The available information is as presented in Table 9.2; note here that the natural

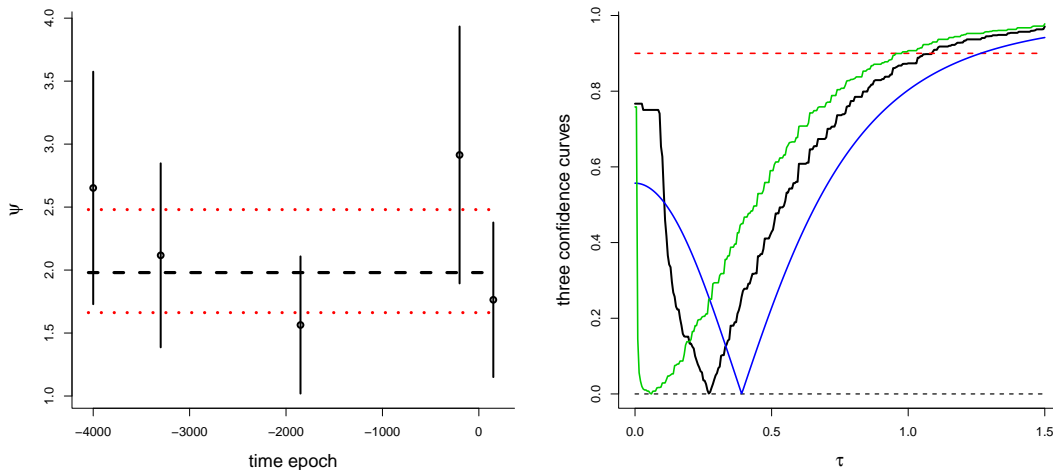


Figure 9.1: Left panel: Point estimates $\hat{\psi}_j$ with 90% confidence intervals, for the skull stretch parameter ψ , across five time epochs (see Table 9.1). Right panel: Three confidence curves for the spread parameter τ , with median confidence estimates 0.006 (the direct profile method), 0.272 (the corrected profile method), 0.390 (the $Q_k(\tau)$ method).

95% confidence interval is not at all symmetric around the point estimate, with an implied skewness to the right.

Table 9.2: Abundance assessment of a humpback population, from 1995 and 2001, summarised as 2.5%, 50%, 97.5% confidence quantiles; from Paxton et al. (2009). See Section 9.2 and Figure 9.2.

	2.5%	50%	97.5%
1995	3439	9810	21457
2001	6651	11319	21214

For this illustration we are interested in the underlying true abundances underlying these two studies. Let ψ_1 be the population size in 1995 and ψ_2 be the size in 2001. Our main interest may lie in the annual growth rate underlying these two population sizes. We define $\rho = (\psi_2 - \psi_1)/(6\psi_1)$, a simple (and in some sense approximate) definition of annual growth rate.

The first step, *Independent Inspection*, requires us to construct CDs for ψ_1 and ψ_2 from the two surveys. In Schweder & Hjort (2016, Ch. 10), certain methods are proposed and developed for constructing CDs based only on an estimate and a confidence interval. With a positive parameter, like abundance, one may use

$$\text{II: } C(\psi_j, y) = \Phi\left(\frac{h(\psi_j) - h(\hat{\psi}_j)}{s}\right)$$

with a power transformation $h(\psi, a) = \text{sgn}(a)\psi^a$; see also Schweder & Hjort (2013) for some more discussion of this approach (along with a different application, essentially also using the II-CC-FF paradigm). In order to estimate the power a and the scale s the following two equations must be solved,

$$\psi_L^a - \hat{\psi}^a = -1.96 s \quad \text{and} \quad \psi_R^a - \hat{\psi}^a = 1.96 s,$$

where $[\psi_L, \psi_R]$ is the 95% confidence interval and $\hat{\psi}$ the median confidence point estimate. For the whale abundance, we find (a, s) equal to $(0.321, 2.798)$ for 1995 and $(0.019, 0.007)$ for 2001 (a small value of a indicates that the transformation is nearly logarithmic). The corresponding confidence curves are shown in the left panel of Figure 9.2. In this case the confidence log-likelihoods in the *Confidence Conversion* step are easily obtained. For year j ,

$$\text{CC:} \quad \ell_{\text{conv},j}(\psi_j) = -\frac{1}{2}\{h_j(\psi_j) - h_j(\hat{\psi}_j)\}^2/s_j^2.$$

In the final *Focused Fusion* step, we sum the two confidence log-likelihoods, profile with respect to ρ , find the combined deviance function, and construct an approximative combined confidence curve by the Wilks theorem, as per Section 2:

$$\begin{aligned} \text{FF:} \quad \ell_{\text{fus,prof}}(\rho) &= \max\{\ell_{\text{conv},1}(\psi_1) + \ell_{\text{conv},2}(\psi_2) : (\psi_2 - \psi_1)/(6\psi_1) = \rho\}, \\ \text{cc}^*(\rho) &= \Gamma_1(2\{\ell_{\text{fus}}(\hat{\rho}) - \ell_{\text{fus}}(\rho)\}). \end{aligned}$$

Here we obtain the blue curve in the right panel of Figure 9.2, with $\hat{\rho} = 0.026$ and a 95% confidence interval $[-0.094, 0.454]$.

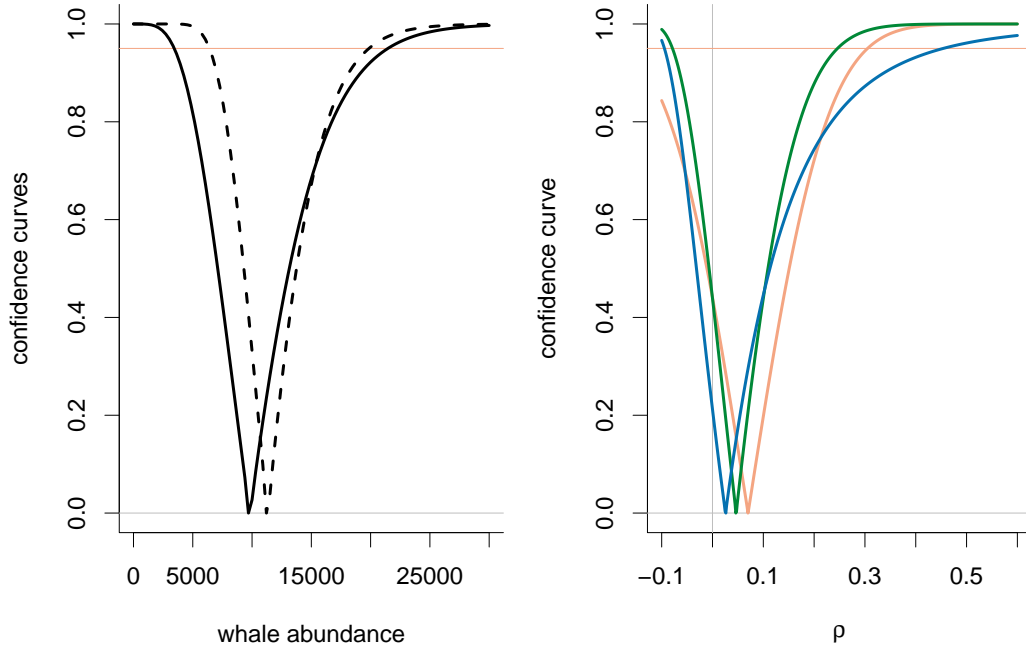


Figure 9.2: Left panel: confidence curves for ψ_1 and ψ_2 , the abundance of humpback whales in the North Atlantic in 1995 (fully drawn line) and 2001 (dashed line). Right panel: the confidence curve for $\rho = (\psi_2 - \psi_1)/(6\psi_1)$ based on the two surveys (blue curve); the confidence curve based on prior information alone (orange curve); and the confidence curve combining the studies and the prior information (green curve). See Section 9.2 and Table 9.2.

In some cases there may exist some expert knowledge pertaining to at least the focus parameter under study, here the annual growth rate ρ , though not necessarily for the full parameter vector of the combined models, here (ψ_1, ψ_2) the two population sizes. A proper Bayesian analysis requires the statistician to have such a prior for (ψ_1, ψ_2) – without this ingredient, there is no Bayes theorem leading to a posterior distribution for the model parameters, or indeed for ρ . The II-CC-FF scheme allows however incorporation of such partial prior information, i.e. a prior for ρ without

a prior for (ψ_1, ψ_2) . For this illustration we assume that whale biologists provide a normal prior with expectation equal to 0.07 and variance 0.12². This prior may come from knowledge of other humpback whale populations or simulation-based life-history models (see for example Zerbini et al. (2010), giving a similar point estimate as we have used).

The prior can be represented as a confidence curve, supplementing the confidence curve based on the two studies. In order to fuse the prior knowledge and the data we simply add the prior log-likelihood $\ell_B(\rho)$ to the confidence log-likelihoods, in the following way,

$$\begin{aligned} \text{FF: } \quad \ell_{\text{fus,prof},B}(\rho) &= \max\{\ell_{\text{conv},1}(\psi_1) + \ell_{\text{conv},2}(\psi_2) + \ell_B(\rho) : (\psi_2 - \psi_1)/(6\psi_1) = \rho\} \\ &= \max_{\sigma_1}\{\ell_{\text{conv},1}(\psi_1) + \ell_{\text{conv},2}(\psi_2) : (\psi_2 - \psi_1)/(6\psi_1) = \rho\} + \ell_B(\rho) \\ &= \ell_{\text{fus,prof}}(\rho) + \ell_B(\rho). \end{aligned}$$

We use ‘B’ as subscript to indicate the in this instance partial and perhaps lazy Bayesian, who does not give a full prior for the model parameters, but contributes a component, namely where it matters the most, about the focus parameter. Of course the log-prior $\ell_B(\rho)$ employed here could have been obtained in the more careful and proper Bayesian way of having started with a full prior for (ψ_1, ψ_2) , and then a transformation, but we do suggest that expert knowledge concerning focus parameters is more often put forward directly, not via the full parameter vector in the fullest model.

Importantly, this extended deviance function does still have an approximate χ_1^2 distribution, by the general approximation arguments briefly discussed in Section 4.3, unless the log-prior $\ell_B(\rho)$ is sharp and distinctly non-normal. One may conceptually and sometimes practically interpret the log-prior as having resulted from real data in previous experiences, in which case the $\ell_B(\rho)$ would be a genuine profiled log-profile likelihood function from such a source. Also, as the sample sizes of the studies increase the information from the two studies will dominate the prior and we can safely continue to use the Wilks theorem. As expected, the confidence curve fusing the prior information and the information from the two studies lies between the original confidence curve and the prior confidence curve (see Figure 9.2, right panel). It is also somewhat narrower than both.

9.3 Olympic medians

This is an Olympic story about certain dynamic changes of the Body Mass Index distribution for speedskaters. We focus specifically on how the median of this distribution has changed over time. Our use of the II-CC-FF scheme will involve first building highly accurate nonparametric CDs for the medians, and then converting these to parametric log-likelihoods, after which a dynamic model for the medians can be fused together in the end. Our methodology will work with modest changes also for cases where interest lies in the evolution of any given quantile, say the 0.90 quantile points of income distributions over time across different strata.

The BMI is defined as weight (in kg) divided by squared height (in metres). Figure 9.3 displays the median BMI, for the male participants, across the ten last Olympics (1984, 1988, 1992, 1994, 1998, 2002, 2006, 2010, 2014, 2018, with the notable breaking of the Olympic rhythm from Albertville to Lillehammer), marked as small red circles. The red line adjoining these sample medians indicates that the BMI has undergone a certain evolution, with a marked increase up to perhaps 1998 Nagano or 2002 Salt Lake City, followed by a downward trend. Even though these changes perhaps do not qualify as drastic, and athletes with 24.5 do not differ very much from those

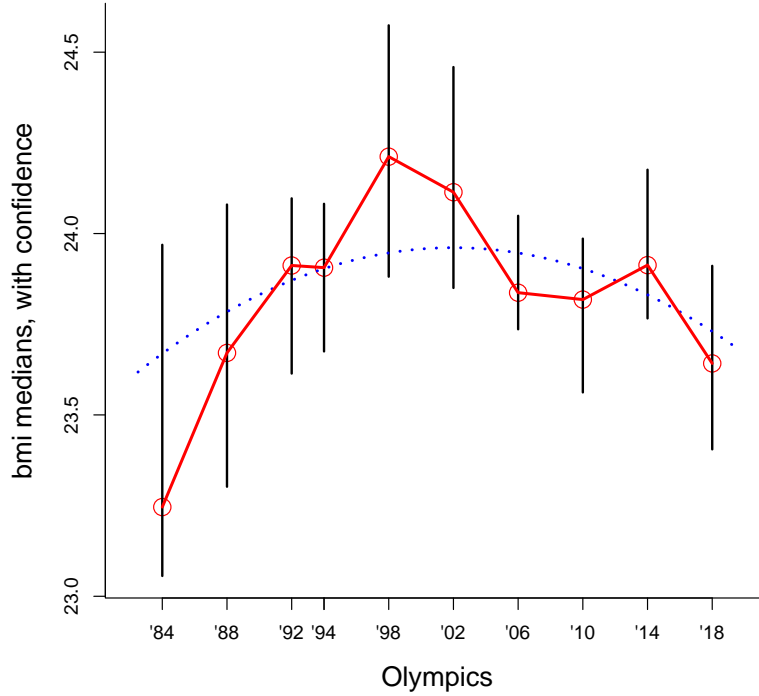


Figure 9.3: Median BMI for men, ten last Olympics 1984 Sarajevo to 2018 Sochi, with 90 percent confidence band, and the fitted parabola (9.1).

with 23.5, they are nevertheless interesting enough to be discussed in the proper fora. Potential underlying reasons behind such an evolution, with an up and a down over ten Olympiads, include (i) the prospect of doping, with building of extra muscle power, etc., and the alleged cleaning of the sport; (ii) the klapskate and the higher speed, which arguable favours technical skills over pure power; and (iii) the introduction of the team event and mass starts, which points to statistical discrepancies in the populations of male Olympic skaters from e.g. 2002 and 2018.

These themes motivate the following investigation, to look both for significant changes and for the position of a potential top-point for the evolution of the BMI distribution over time. Let μ_j be the population median at Olympics j , for occasions $j = 1, \dots, k$. We first need CDs for these, constructed nonparametrically. With $y_{j,(1)} < \dots < y_{j,(n_j)}$ the ordered sample from Olympics j , assumed to come from a continuous distribution with positive density f_j and cumulative F_j , we start from the exact calculation

$$P_{f_j}\{\mu_j \leq y_{j,(r)}\} = P\{F_j(\mu_j) \leq F_j(y_{j,(r)})\} = P\{\frac{1}{2} \leq U_{j,(r)}\},$$

with $U_{j,(1)} < \dots < U_{j,(n_j)}$ an ordered i.i.d. sample from the uniform distribution on the unit interval. But these have known Beta distributions. We therefore define the $C_j(\mu_j)$ for all values of μ_j by first setting

$$C_j(y_{j,(r)}) = 1 - \text{Be}(\frac{1}{2}, r, n_j - r + 1) \quad \text{for } r = 1, \dots, n_j,$$

featuring cumulative Beta distribution functions, and then applying linear interpolation between the ordered data points. The full confidence curves $cc_j(\mu_j) = |1 - 2C_j(\mu_j)|$ are displayed in

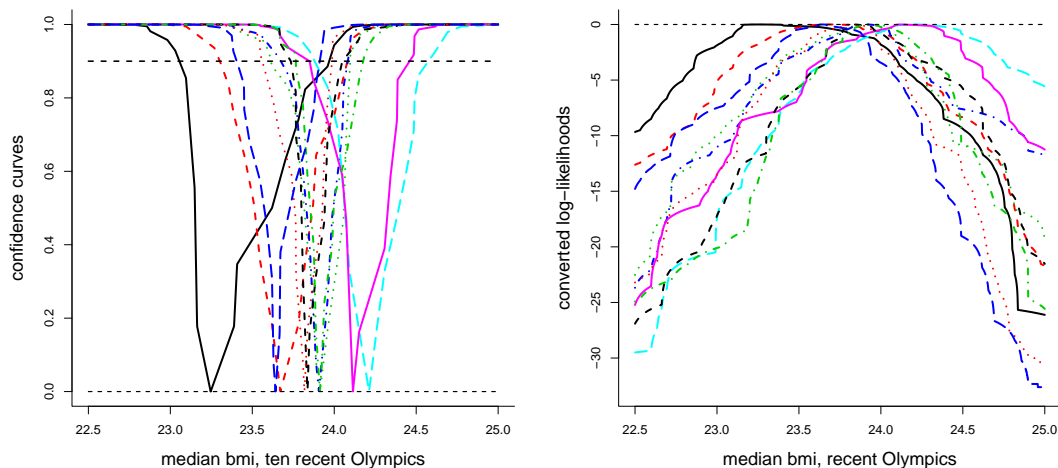


Figure 9.4: Left: Nonparametric confidence curves $cc_j(\mu_j)$ for the medians of the BMI distributions, for the ten last Olympics 1984 to 2018. 90 percent confidence intervals are read off from the horizontal dashed line at 0.90. Right: Converted log-likelihood contributions $\ell_{\text{conv},j}(\mu_j)$ for the ten Olympic medians.

Figure 9.4 (left panel) and they are then converted to log-likelihood components $\ell_{\text{conv},j}(\mu_j) = -\frac{1}{2}\Gamma_1^{-1}(cc_j(\mu_j))$ (right panel). The 90 percent confidence intervals for the ten medians shown in Figure 9.3 are computed from the $cc_j(\mu_j)$. Note that these confidence curves and intervals are fully nonparametric. They can be shown to be highly accurate, even for smaller sample sizes, and work better than alternative methods involving approximate normality with estimates of standard errors. The resulting intervals deviate from symmetry, reflecting underlying asymmetry in the distribution of the BMI.

Next we model the medians μ_j dynamically as

$$\mu_j = \beta_0 + \beta_1 x_j + \beta_2 x_j^2 \quad \text{for } j = 1, \dots, k, \quad (9.1)$$

where $x_j = t_j - t_1$ is the time passed since the first of the Olympics to no. j . Such a model is found to be entirely adequate via AIC analysis. The parameters of this parabola will be such that it has a maximum point

$$x^* = x^*(\beta_0, \beta_1, \beta_2) = -\beta_1/(2\beta_2) \quad (9.2)$$

within the range from the first to the last of these Olympics, see again Figure 9.3. Now the FF step of our general recipe leads to $\ell_{\text{fus}}(\beta_0, \beta_1, \beta_2) = -\frac{1}{2} \sum_{j=1}^k \Gamma_1^{-1}(cc_j(\beta_0 + \beta_1 x_j + \beta_2 x_j^2))$, and then to the profiled version

$$\ell_{\text{fus}}(x^*) = \max\{\ell_{\text{fus}}(\beta_0, \beta_1, \beta_2) : (\beta_0, \beta_1, \beta_2) \text{ fitting with } x^*\}.$$

Using the FF step of our II-CC-FF is also equivalent to working with the fused deviance function $D_{\text{fus}}(x^*) = 2\{\ell_{\text{fus}}(\hat{x}^*) - \ell_{\text{fus}}(x^*)\}$, with \hat{x}^* the appropriate function of the overall maximisers of $\ell_{\text{fus}}(\beta_0, \beta_1, \beta_2)$.

Carrying out this machinery leads first to the fitted parabola shown as the blue dashed curve in Figure 9.3. The linear and quadratic coefficients β_1 and β_2 are very significantly positive and negative, respectively, as shown via Wald ratios; also, the estimated top-point is at $\hat{x}^* = 2002.4$.

Secondly, using the distribution approximation $D_{\text{fus}}(x^*) \sim \chi_1^2$ we can execute the FF step and compute the confidence curve $cc_{\text{fus}}(x^*) = \Gamma_1(D_{\text{fus}}(x^*))$. It is displayed in Figure 9.5, with the partial ruggedness and asymmetry reflecting the nonsmoothness of the ten nonparametric sample median operations. We have been able to use confidence conversion, from nonparametric confidence curves to log-likelihood contributions and then back again to a focused fusion confidence curve. The 90 percent confidence interval for the point of maximum median BMI for male speedskaters is from 1992.1 to 2009.7.

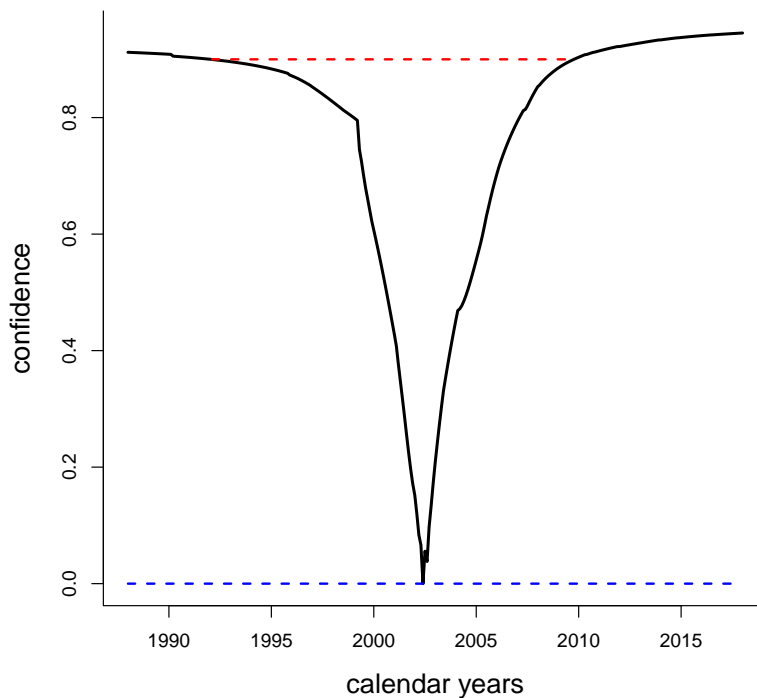


Figure 9.5: Focused Fusion confidence curve for $x^* = -\beta_1/(2\beta_2)$, the maximum point for the parabola in the model for Olympic BMI medians.

9.4 The long peace

Our last illustration concerns the use of the II-CC-FF framework in a highly non-standard setting, where one wishes to combine hard data, sources that inform directly on the focus parameter, with softer data sources, which only contain indirect or noisier information about the focus parameter. This kind of combination has wide potential in various fields where ‘soft’ data could be based on webscraping, using twitter accounts or other social media, but raises specific issues and challenges. The question we investigate here is the extent of statistical evidence for The long peace, the period of relative peace and stability following the second world war (and still lasting, presumably). Specifically, do we find evidence of a change-point τ when analysing the sequence of battle deaths in interstate wars between 1823 and today?

There are many components, issues, and details involved in this application story, and a fuller version is reported on in Appendix B. Here we outline the main statistical ingredients. First,

the question has been investigated in Cunen, Hjort & Nygård (2020) using the Correlates of War (CoW) dataset (Sarkees & Wayman, 2010). The authors found evidence of an abrupt change in the battle death distribution at some point after the second world war, from a distribution with a high median battle death to a distribution with a lower median (and also a less heavy tail). This involved establishing a certain three-parameter model for the battle deaths distribution, with parameters changing at time τ , itself an unknown change-point parameter. We may view the relevant statistical information as represented by an FF based log-likelihood contribution $\ell_{B,\text{prof}}(\tau)$. Here the aim is to extend this analysis and investigate whether there might be benefits in combining the battle death data with other sources assumed to be informing on τ .

Some political scientists consider the aforementioned decrease in battle deaths to reflect a moral and political shift within a large portion of the world’s population. At some point in the 20th century, it is argued, the perception of war changed, from being seen as something natural and inevitable, sometimes even positive, to being perceived as highly negative, evil and unacceptable; cf. Pinker (2011, Ch. 5). This change in norms has likely manifested itself in various ways, including cultural, artistic and political expressions, for example through text. We have therefore collected sequences representing the usage of certain relevant words or phrases, like ‘anti-war’ or ‘pacifist’, and then attempted to combine the change-point inference from such an Ngram analysis (suggested to us by Steven Pinker, personal communication), with the change-point inference from the battle deaths data. Such statistical work, along with data collection and separate modelling efforts, leads to an overall log-likelihood contribution $\ell_{N,\text{prof}}(\tau)$ for the potential change-point τ . These combination efforts lead to an overall log-likelihood fusion function

$$\ell_{\text{fus}}(\tau) = w_B \ell_{B,\text{prof}}(\tau) + w_N \ell_{N,\text{prof}}(\tau),$$

with relative importance weights w_B and w_N , involving a separate discussion. Other applications, involving the combination of perhaps very different data sources, would similarly involve separate and perhaps partly subjective analyses for deciding on such relative importance weight parameters. For the present application, with battle deaths the hard data and Ngrams the soft data, more details are presented in Appendix B, along with our tentative concluding confidence curve $cc^*(\tau)$.

Acknowledgements. The work reported on here has been partially funded via the Norwegian Research Council’s project *FocuStat: Focused Statistical Inference With Complex Data*, led by Hjort. The authors are grateful to comments from Steven Pinker, and to Tore Schweder and Emil Stoltenberg for always fruitful discussions related to issues and methods worked with in this paper. Constructive comments and suggestions from anonymous reviewers and an associate editor have contributed to a better paper. The data on heights and weights and hence BMI for Olympic speedskaters stem from files collected over the years by N.L.H., and in this endeavour he has been helped by fellow speedskating historians Arild Gjerde and Jeroen Heijmans.

References

- BARNDORFF-NIELSEN, O. E. (1986). Inference on full or partial parameters based on the standardized signed log likelihood ratio. *Biometrika* **73**, 307–322.
- BERGER, J. O., LISEO, B. & WOLPERT, R. L. (1999). Integrated likelihood methods for eliminating nuisance parameters [with discussion]. *Statistical Science* **14**, 1–28.
- BRESLOW, N. (1981). Odds ratio estimators when the data are sparse. *Biometrika* **68**, 73–84.

- CAI, T., PARAST, L. & RYAN, L. (2010). Meta-analysis for rare events. *Statistics in Medicine* **29**, 2078–2089.
- CHADEFAUX, T. (2014). Early warning signals for war in the news. *Journal of Peace Research* **51**, 5–18.
- CHENG, J. Q., LIU, R. Y. & XIE, M.-G. (2017). Fusion learning. *Wiley StatsRef: Statistics Reference Online* .
- CLAESKENS, G. & HJORT, N. L. (2008). *Model Selection and Model Averaging*. Cambridge: Cambridge University Press.
- COX, D. R. & REID, N. (1987). Parameter orthogonality and approximate conditional inference [with discussion]. *Journal of the Royal Statistical Society, Series B* **49**, 1–39.
- COX, D. R. & REID, N. (1993). A note on the calculation of adjusted profile likelihood. *Journal of the Royal Statistical Society, Series B* **55**, 467–471.
- CUNEN, C., HERMANSEN, G. & HJORT, N. L. (2018). Confidence distributions for change-points and regime-shifts. *Journal of Statistical Planning and Inference* **195**, 14–34.
- CUNEN, C. & HJORT, N. L. (2015). Optimal inference via confidence distributions for two-by-two tables modelled as Poisson pairs: fixed and random effects. In *Proceedings 60th World Statistics Congress, 26-31 July 2015, Rio de Janeiro*, vol. I. Amsterdam: International Statistical Institute, pp. 3581–3586.
- CUNEN, C., HJORT, N. L. & NYGÅRD, H. M. (2020). Statistical sightings of better angels: analysing the distribution of battle-deaths in interstate conflict over time. *Journal of Peace Research* **57**, 221–234.
- DICICCIO, T. & EFRON, B. (1992). More accurate confidence intervals in exponential families. *Biometrika* **79**, 231–245.
- DICICCIO, T. J., MARTIN, M. A., STERN, S. E. & YOUNG, G. A. (1996). Information bias and adjusted profile likelihoods. *Journal of the Royal Statistical Society, Series B* **58**, 189–203.
- DOMINICI, F. & PARMIGIANI, G. (2000). Combining studies with continuous and dichotomous responses: A latent-variables approach. In *Meta-analysis in Medicine and Health Policy*. CRC Press, pp. 99–118.
- DURBAN, M. & CURRIE, I. D. (2000). Adjustment of the profile likelihood for a class of normal regression models. *Scandinavian Journal of Statistics* **27**, 535–542.
- EFRON, B. (1993). Bayes and likelihood calculations from confidence intervals. *Biometrika* **80**, 3–26.
- EFRON, B. & HASTIE, T. (2016). *Computer Age Statistical Inference*. Cambridge: Cambridge University Press.
- FERGUSON, T. S. (1996). *A Course in Large Sample Theory*. Los Angeles: Chapman & Hall.
- FISHER, R. A. (1954). *Statistical Methods for Research Workers*. London: Oliver & Body.
- GADDIS, J. L. (1989). *The Long Peace: Inquiries Into the History of the Cold War*. Oxford: Oxford University Press.
- HARDY, R. J. & THOMPSON, S. G. (1996). A likelihood approach to meta-analysis with random effects. *Statistics in Medicine* **15**, 619–629.
- HJORT, N. L. & SCHWEDER, T. (2018). Confidence distributions and related themes [introduction to the special issue, by the guest editors]. *Journal of Statistical Planning and Inference* **195**, 1–13.
- JACKSON, D., LAW, M., STIJNEN, T., VIECHTBAUER, W. & WHITE, I. R. (2018). A comparison of seven random-effects models for meta-analyses that estimate the summary odds ratio. *Statistics in Medicine* **37**, 1059–1085.
- KRISTENSEN, K., NIELSEN, A., BERG, C., SKAUG, H. & BELL, B. (2016). TMB: Automatic differentiation and Laplace approximation. *Journal of Statistical Software* **70**, 1–21.
- LANGAN, D., HIGGINS, J. P., JACKSON, D., BOWDEN, J., VERONIKI, A. A., KONTOPANTELOS, E., VIECHTBAUER, W. & SIMMONDS, M. (2019). A comparison of heterogeneity variance estimators in simulated random-effects meta-analyses. *Research Synthesis Methods* **10**, 83–98.

- LIU, D., LIU, R. & XIE, M.-G. (2014a). Exact inference methods for rare events. *Wiley StatsRef: Statistics Reference Online*, 1–6.
- LIU, D., LIU, R. Y. & XIE, M.-G. (2014b). Exact meta-analysis approach for discrete data and its application to 2×2 tables with rare events. *Journal of the American Statistical Association* **109**, 1450–1465.
- LIU, D., LIU, R. Y. & XIE, M.-G. (2015). Multivariate meta-analysis of heterogeneous studies using only summary statistics: Efficiency and robustness. *Journal of the American Statistical Association* **110**, 326–340.
- MANTEL, N. & HAENSZEL, W. (1959). Statistical aspects of the analysis of data from retrospective studies of disease. *Journal of the National Cancer Institute* **22**, 719–748.
- MCCULLAGH, P. & TIBSHIRANI, R. (1990). A simple method for the adjustment of profile likelihoods. *Journal of the Royal Statistical Society. Series B* **52**, 325–344.
- MICHEL, J.-B., SHEN, Y. K., AIDEN, A. P., VERES, A., GRAY, MATTHEW K BROCKMAN, W., THE GOOGLE BOOKS TEAM, PICKETT, J. P., HOIBERG, D., CLANCY, D., NORVIG, P., ORWANT, J., PINKER, S., NOWAK, M. A. & AIDEN, E. L. (2010). Quantitative analysis of culture using millions of digitized books. *Science* **331**.
- NOMA, H. (2011). Confidence intervals for a random-effects meta-analysis based on Bartlett-type corrections. *Statistics in Medicine* **30**, 3304–3312.
- O’ROURKE, K. (2008). *The Combining of Information: Investigating and Synthesizing What is Possibly Common in Clinical Observations or Studies Via Likelihood*. Ph.D. thesis, University of Oxford.
- PARTLETT, C. & RILEY, R. D. (2017). Random effects meta-analysis: Coverage performance of 95% confidence and prediction intervals following REML estimation. *Statistics in Medicine* **36**, 301–317.
- PAXTON, C. G. M., BURT, M. L., HEDLEY, S. L., VÍKINGSSON, G. A., GUNNLAUGSSON, T. & DESPORTES, G. (2009). Density surface fitting to estimate the abundance of Humpback whales based on the NASS-95 and NASS-2001 aerial and shipboard surveys. *NAMMCO Scientific Publications* **7**, 143–160.
- PIAGET-ROSSEL, R. & TAFFÉ, P. (2019). Meta-analysis of rare events under the assumption of a homogeneous treatment effect. *Biometrical Journal* **61**, 1557–1574.
- PINKER, S. (2011). *The Better Angels of Our Nature: Why Violence Has Declined*. Toronto: Viking Books.
- ROTHMAN, K. J., GREENLAND, S. & LASH, T. L. (2008). *Modern epidemiology*. Lippincott Williams & Wilkins.
- SARKEES, M. R. & WAYMAN, F. W. (2010). *Resort to War: a Data Guide to Inter-state, Extra-state, Intra-state, and Non-state Wars, 1816-2007*. Washington, DC: CQ Press.
- SCHWEDER, T. & HJORT, N. L. (2013). Integrating confidence intervals, likelihoods and confidence distributions. In *Proceedings 59th World Statistics Congress, 25-30 August 2013, Hong Kong*, vol. I. Amsterdam: International Statistical Institute, pp. 277–282.
- SCHWEDER, T. & HJORT, N. L. (2016). *Confidence, Likelihood, Probability: Statistical Inference with Confidence Distributions*. Cambridge: Cambridge University Press.
- SIMMONDS, M. C. & HIGGINS, J. P. (2016). A general framework for the use of logistic regression models in meta-analysis. *Statistical Methods in Medical Research* **25**, 2858–2877.
- SIMPSON, R. J. S. & PEARSON, K. (1904). Report on certain enteric fever inoculation statistics. *The British Medical Journal* **3**, 1243–1246.
- SINGH, K., XIE, M.-G. & STRAWDERMAN, W. E. (2005). Combining information from independent sources through confidence distributions. *Annals of Statistics* **33**, 159–183.
- STERN, S. E. (1997). A second-order adjustment to the profile likelihood in the case of a multidimensional parameter of interest. *Journal of the Royal Statistical Society, Series B* **59**, 653–665.
- STIJNEN, T., HAMZA, T. H. & ÖZDEMİR, P. (2010). Random effects meta-analysis of event outcome in the framework of the generalized linear mixed model with applications in sparse data. *Statistics in Medicine* **29**, 3046–3067.

- THOMSON, A. & RANDALL-MACIVER, R. (1905). *Ancient Races of the Thebaid: Being an Anthropometrical Study of the Inhabitants of Upper Egypt from the Earliest Prehistoric Times to the Mohammedan Conquest, Based Upon the Examination of Over 1,500 Crania*. Oxford: Oxford University Press.
- VAN HOUWELINGEN, H. C., ZWINDERMAN, K. H. & STIJNEN, T. (1993). A bivariate approach to meta-analysis. *Statistics in Medicine* **12**, 2273–2284.
- VIECHTBAUER, W. (2010). Conducting meta-analyses in R with the metafor package. *Journal of Statistical Software* **36**, 1–48.
- WHITEHEAD, A., BAILEY, A. J. & ELBOURNE, D. (1999). Combining summaries of binary outcomes with those of continuous outcomes in a meta-analysis. *Journal of Biopharmaceutical Statistics* **9**, 1–16.
- XIE, M., SINGH, K. & STRAWDERMAN, W. E. (2011). Confidence distributions and a unifying framework for meta-analysis. *Journal of the American Statistical Association* **106**, 320–333.
- XIE, M.-G. & SINGH, K. (2013). Confidence distribution, the frequentist distribution estimator of a parameter: A review [with discussion and a rejoinder]. *International Statistical Review* **81**, 3–39.
- YANG, G., SHI, P. & XIE, M.-G. (2016). *gmeta: Meta-Analysis via a Unified Framework of Confidence Distribution*. R package version 2.2-4.
- YU, Y. & TIAN, L. (2014). *exactmeta: Exact fixed effect meta analysis*. R package version 1.0-2.
- ZERBINI, A. N., CLAPHAM, P. J. & WADE, P. R. (2010). Assessing plausible rates of population growth in humpback whales from life-history data. *Marine Biology* **157**, 1225–1236.

Below follow extra material, organised as Appendixes A, B, C. The first gives more details pertaining to our simulations, summarised in Section 8. Appendix B reports on our study of how to combine hard data (battle death counts, for 95 major wars) and soft data (Ngram monitoring studies for certain key-words, sampled from tens of millions of books). Finally details for how the II-CC-FF deals with the Neyman–Scott situation are in Appendix C.

A Additional details on the simulations

Here we provide some more details on the simulations presented in Sections 8.1 and 8.2. In particular, we provide the R function calls for the methods with which we have compared our II-CC-FF methods. For Section 8.2 we also present some additional results which were described in the text.

A.1 The basic random effect model

For the Hartung–Knapp–Sidik–Jonkman method we used the implementation in the `metafor` package, and the following function call

```
rma.uni(yi= sumM[,1], sei= sumM[,2], test="knha")
```

The matrix `sumM` provides the k estimates for ψ_j in the first column, and estimates for σ_j in the second. With this function, the default estimator for τ is the REML estimator. Note that there is a small probability that this function fails if the algorithm for finding the REML estimator does not converge, and in those (very few) cases we used the DerSimonian–Laird method instead.

For the CD combination method of Xie et al. (2011), we used the implementation in the `gmeta` package,

```
gmeta(sumM[,1:2], method="random-reml", gmo.xgrid=psival)
```

The matrix `sumM` provides the k estimates for ψ_j in the first column, and estimates for σ_j in the second. The vector `psival` is a grid of 500 values for ψ_0 (but with limits adjusted according to k and τ). This was the same grid we used for our II-CC-FF methods. With this function, the default estimator for τ is the REML estimator. Note that there is a somewhat significant probability that this function fails if the algorithm for finding the REML estimator does not converge, and in those cases we used the DerSimonian-Laird method instead. The option `method="random-reml"` is actually one of six choices for the basic random effect model which are implemented in the `gmeta` package. We did not find any recommendations concerning which method to choose, except that we avoided the methods denoted as `"robust"`, since these are meant for situations where there are outlying studies, according to Xie et al. (2011) (and which is not the case in our set-up).

A.2 Meta-analysis of 2×2 tables

For the fixed effect meta-analysis we used the Mantel-Haenszel method which we implemented ourselves based on the formulas given in Piaget-Rossel & Taffé (2019). For the variance of the estimator of the risk difference (equation (19) in Piaget-Rossel & Taffé (2019)) there seemed to be a small typo, and we replaced the minus sign in the middle with a plus sign.

Note that for the odds ratio and risk ratio, the Mantel-Haenszel method produces indefinite estimates when there is not a single event in the entire control arm of a study (i.e. all $y_{0,j}$ are equal to zero). The `gmeta` also fails in this situation, which happens occasionally in the set-up shown in Figure 8.2: in 7% of the rounds for $k = 5$ for instance. For the sake of fair comparisons we have removed these rounds from all the methods. Further, the Mantel-Haenszel produces indefinite variance estimates also when there is not a single event in the entire treatment arm of a study (i.e. all $y_{1,j}$ are equal to zero). This situation happens often in our set-up (around 50% of the time for $k = 5$) and in these cases we defined the 95% confidence interval from the Mantel-Haenszel method as spanning the entire real line. The II-CC-FF methods never fail/crash: in situations with zero events in the entire control arm or the entire treatment arm, the resulting confidence curves for the log odds ratio (or the log risk ratio) will have a point-mass in infinity or minus infinity, respectively.

We used the `gmeta` package for the odds ratio and the risk difference. With the following function calls,

```
gmeta(dd,gmi.type="2x2", method="exact1")
gmeta(dd,gmi.type="2x2", method="exact2")
```

The matrix `dd` has k rows and four columns. The first and third column are the number of events in treatment and control group respectively. The second and fourth column are the sample sizes in each group. The options `"exact1"` and `"exact2"` are chosen according to the `gmeta` documentation.

For the risk ratio we used the `exactmeta` package with the following function call,

```
meta.exact(dd[,c("y0","y1","m0","m1")], type="rate ratio", print=F)
```

Note here that we used the `"rate ratio"` option which actually computes the ratio of two Poisson rates. There exists an option `"risk ratio"` in the package, but that option was prohibitively slow. When event probabilities are small the Poisson rates and binomial proportions will be close

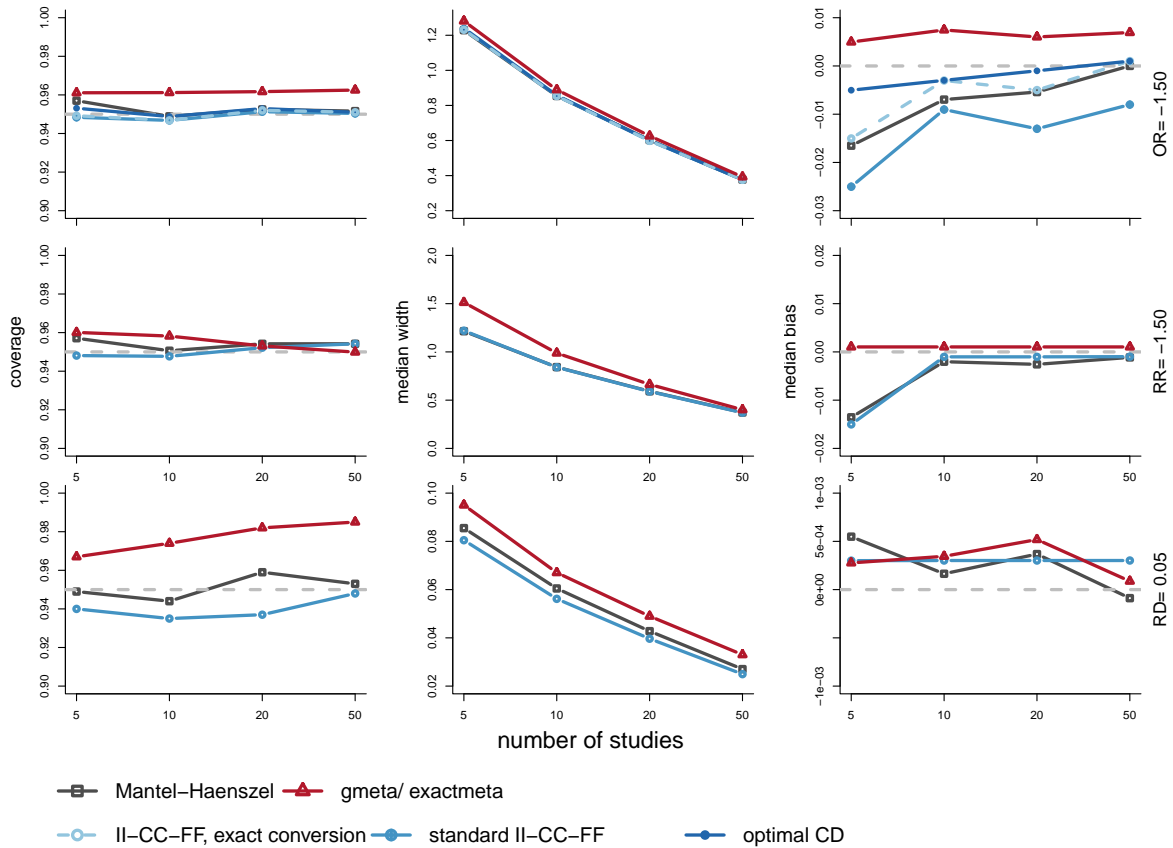


Figure A.1: Simulation results for fixed effect meta-analysis of 2×2 tables in a setting with not particularly rare events. The left column gives the realised coverage rate of 95% confidence intervals, the middle column gives the median width of these intervals and the right column gives the median bias of the point estimate coming from each of the methods. The top row gives the results for the (log) odds ratio, the middle row for the (log) risk ratio and the bottom row gives the results for the risk difference.

to equal. If anything we are giving the `exactmeta` package an edge compared to the other methods here.

As mentioned in Section 8.2 we have run similar simulations as the ones shown there, but in a setting with less rare events. These results are shown in Figure A.1. There we have median event probability in the control group is 0.1, instead of 0.005 in the main text.

Here we also provide two additional notes on the methods we have used and the links between them. (1) For the odds ratio, the Liu et al. (2014a) method, the optimal CD method and the II-CC-FF method with exact conversion are all three closely related to the Fisher exact test (Fisher, 1954). Their performance is very different, however, and that is due to different strategies for the combination of the information from each source. (2) Piaget-Rossel & Taffé (2019) report that the estimators from the Mantel- Haenszel procedure correspond to their respective maximum likelihood estimators when the sample sizes in the two groups have a constant ratio for all studies. We have simulated data where we allow for some variability in the ratio between the sample sizes, but this might still constitute a partial explanation for why our II-CC-FF methods have relatively similar behaviour as the Mantel-Haenszel method.

For the random effects simulations, we compared our methods with the modified Simmonds-Higgins method. The method is implemented in the `metafor` package, and we used the following

function call

```
rma.glmm(measure="OR",ai=y1sim,bi=m1s-y1sim,ci=y0sim,di=m0s-y0sim,model="UM.FS")
```

The vectors `y1sim`, `m1s-y1sim`, `y0sim`, and `m0s-y0sim` are all k -dimensional and represent the number of events and non-events in the treatment and control group, respectively. The option "UM.FS" denotes the modified Simmonds-Higgins method.

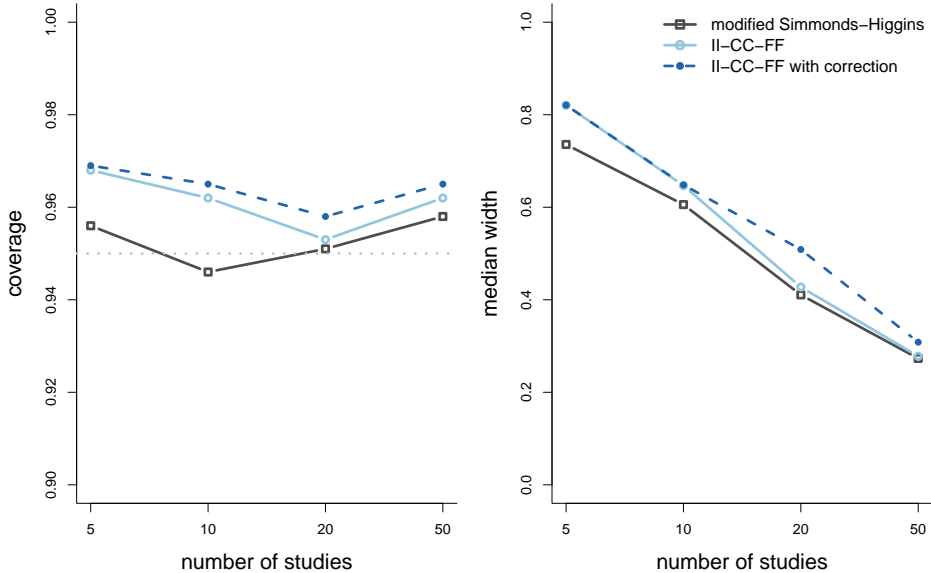


Figure A.2: Simulation results for random effect meta-analysis of 2×2 tables with little heterogeneity in the treatment effects. The left plot gives the realised coverage rate of 95% confidence intervals, the right plot gives the median width of these intervals.

As mentioned in Section 8.2 we have run similar simulations as the ones shown there, but in a setting with little heterogeneity in the treatment effects. These results are shown in Figure A.2. There we have used $\tau = \sqrt{0.024}$ (instead of $\tau = \sqrt{0.168}$ in the main text). We have furthermore also increased the sample sizes, with $m_{1,j} \sim \text{unif}(10, 100)$.

B Combining hard and soft data: battle deaths and Ngrams

Here we provide more details for Application 9.4. The grand but imprecisely posed statistical meta-question to be addressed is whether the world is experiencing something worthy of being called *The long peace*, see Gaddis (1989) and the long chapter in Pinker (2011) for extensive discussions; whether a change-point from ‘before’ to ‘after’ may be identified; and in that case with what precision. The ‘hard data’ to be used are from data source (B), say, the series of battle deaths for the 95 major interstate wars, from 1823 to the present, with at least 1000 deaths. This is to be combined with ‘soft data’ from data source (N), what we might find via the Google Books Ngram Viewer machinery (Michel et al., 2010), monitoring the changes and evolution over time regarding the frequency with which certain words or key phrases are used in tens of millions of books, with corpora currently spanning the era from 1800 to 2010.

These questions have already been addressed in Cunen, Hjort & Nygård (2020), using then only the hard data (B). They developed the three-parameter model with cumulative distribution

function

$$F(z, \mu, \alpha, \theta) = \left[\frac{\{(z - 1000)/\mu\}^\theta}{1 + \{(z - 1000)/\mu\}^\theta} \right]^\alpha \quad \text{for } z \geq 1000,$$

which has the type of heavy tails seen in various analyses of such violence data. It was demonstrated first that the battle deaths series has not been constant over time, and then that there is an identifiable change-point τ , with one parameter vector before and another parameter vector after τ . Their point estimate is 1950, the Korean war, and the authors constructed a full confidence curve, say $cc_B(\tau)$, for the change-point, using methodology developed in Cunen, Hermansen & Hjort (2018). These methods do employ log-likelihood profiling, so there is indeed an $\ell_{B,\text{prof}}(\tau)$ involved, though distributions of deviance functions are far from chi-squared; also, the resulting confidence sets might be unions of disjoint intervals. This aspect of such confidence methods for change-points is seen in Figure B.2. The curve reveals a point estimate for the change-point in 1950, but with considerable uncertainty; the years 1939 and 1965 are also considered likely candidates for the change.

We will now discuss how to arrive at a supplementary $\ell_{N,\text{prof}}(\tau)$ using Ngram counts, which warrants a separate brief detour in our statistical discussion. Some political scientists consider the aforementioned decrease in battle deaths to reflect a moral and political shift within a large portion of the world’s population. At some point in the 20th century, it is argued, the perception of war changed, from being seen as something natural and inevitable, sometimes even positive, to being perceived as highly negative, evil, and unacceptable; cf. Pinker (2011, Ch. 5). This change in norms has likely manifested itself in various ways, including cultural, artistic and political expressions, for example through text. We will therefore collect sequences representing the usage of certain relevant words, and then attempt to combine the change-point inference from such an Ngram analysis (suggested to us by Steven Pinker, personal communication), with the change-point inference from the battle deaths data.

We aim at providing a more thorough analysis of these questions in future work, also factoring in yet other information sources; ‘signals for war’ indexes of the type worked with in Chadefaux (2014), perhaps assisted by machine learning algorithms to sample news sources from around the world and reading their pre-war-signals, would be worthwhile to include. For the sake of the present illustration we limit ourselves to Ngram analysis of one word, however: ‘anti-war’. We collected the rate of usage of ‘anti-war’ for each year between 1823 and 2003 from the Ngram viewer, see Figure B.1. The rate of usage is the number of times that word appears in each year divided by the total number of words in the Google Books corpus from each year. For a more thorough analysis we would build a score based on several such Ngrams, or even a joint model for several Ngrams, but those efforts are outside the scope of this illustration. Naturally, the whole analysis rests upon a strong assumption: that the change-point parameter underlying the sequence of battle-deaths and the (potential) change-point parameter underlying the Ngram are somehow the same parameter. We thus assume that changes in the battle death distribution and in the ‘anti-war’ distribution are two different manifestations of the same underlying process.

We model the ‘anti-war’ Ngram with a simple normal model with an autoregressive correlation structure of order 1. We allow the change-point to influence both the expectation and variance parameters of the model, but it turns out that it is primarily the expectation that changes across the change-point (it increases). The correlation between consecutive years is high (0.80). From Figure B.1 it is clear that there are at least one very clear change-point in the sequence of usage

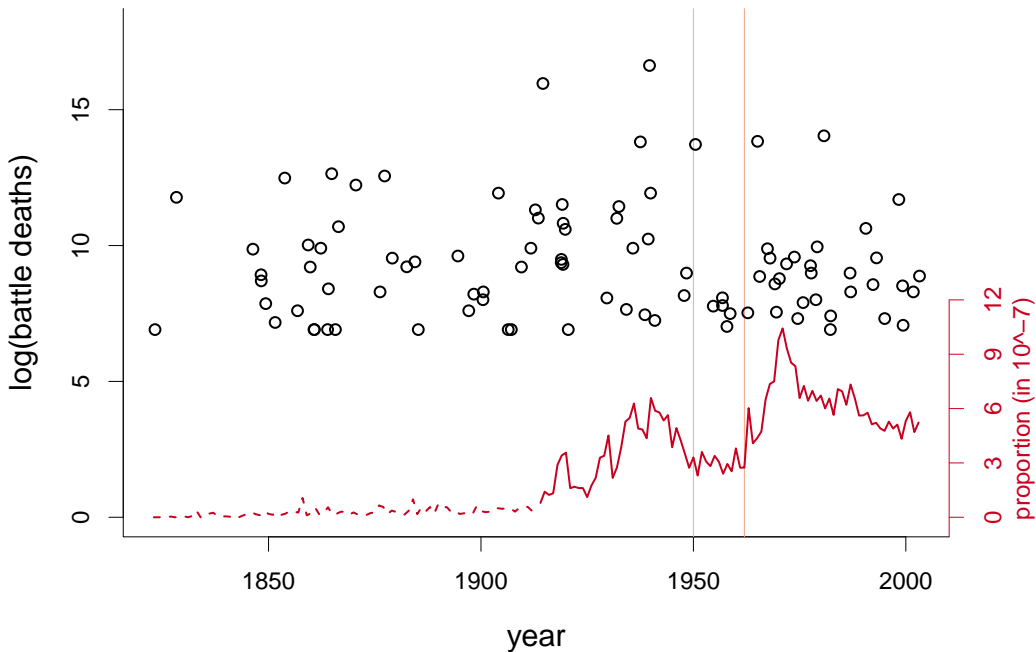


Figure B.1: The points represent the battle deaths, on log scale, for 95 wars between 1823 and 2003. Note that the CoW dataset only includes wars with at least 1000 battle deaths. The vertical grey line gives the point estimate for the change-point based on the battle deaths data. The red line shows the Ngram for ‘anti-war’, i.e. the number of times that word appears in each year divided by the total number of words in the corpus from each year. The counts between 1823 and 1913 were not used in the change-point analysis (and hence dashed). The vertical red line gives the point estimate for the change-point based on the Ngram.

rates: from 1823 to 1914 ‘anti-war’ is hardly used at all (dashed line in the figure), and then the use increases. This increase might reflect a genuine increase in usage, or simply that the Google Books corpus is less complete for older texts. At any rate, we will assume that the change-point around 1914 (from no use to some use) is not the one we are interested in, but rather that the change in norms we are searching for must be reflected in a potential later change-point (from some use to more use). We will therefore only use the Ngram data for the years after 1914; one must bear in mind that this entails that the Ngram can only influence the change-point inference for the latter part of the full sequence of war years.

Using the autoregressive model and the method from Cunen, Hermansen & Hjort (2018), we obtain another log-likelihood profile $\ell_{N,\text{prof}}(\tau)$ and also the full confidence curve based on the Ngram information (in blue in the left panel of Figure B.2). This curve has a point estimate at 1962, but with considerable confidence for the change rather taking place in 1927, or in 1971.

In the fusion step, the most straightforward solution is simply to sum the two log-likelihood profiles, calculate the deviance, and run the simulations to find the distribution of the deviance at each potential change-point (in the way as described in Cunen, Hermansen & Hjort (2018)). This raises the question on whether it is appropriate to treat the two sources of information equally, however. There could be good reasons to consider the battle death data to be more directly informative for τ than the ‘anti-war’ data. These arguments invite a combined confidence log-

likelihood of the form

$$\text{FF: } \ell_{\text{fus}}(\tau) = w_B \ell_{B,\text{prof}}(\tau) + w_N \ell_{N,\text{prof}}(\tau),$$

with weight factors w_B, w_N reflecting the relative importance attached to the N source of information compared to the B source. In the optimistic case where the two sources are seen to inform on the same parameter in equal measure, the weights are set to 1. In most situations there might be no direct information available which could help one estimate these importance-or-relevance weights. In cases where these weights are set by the analyst, the effect of the choice should be communicated clearly and openly. This is also related to difficult themes of what might be seen as a meaningful proxy for what.

In the right panel of Figure B.2 we display the confidence curve with balance parameters $(1, 0.2)$ (in light violet), along with the curve without down-weighting of the soft data, i.e. weights $(1, 1)$ (in dark violet). Both combined curves indicate a point estimate of 1965; this was not the point estimate in any of the two sources, but that year has a high confidence in both. The combined curve with equal balancing gives the appearance of higher precision than the light violet curve, but this might be misleading if we do not trust the ‘soft data’ fully. Then we might prefer the combined curve with weights $(1, 0.2)$, which is more similar to the original curve based on the battle death information only.

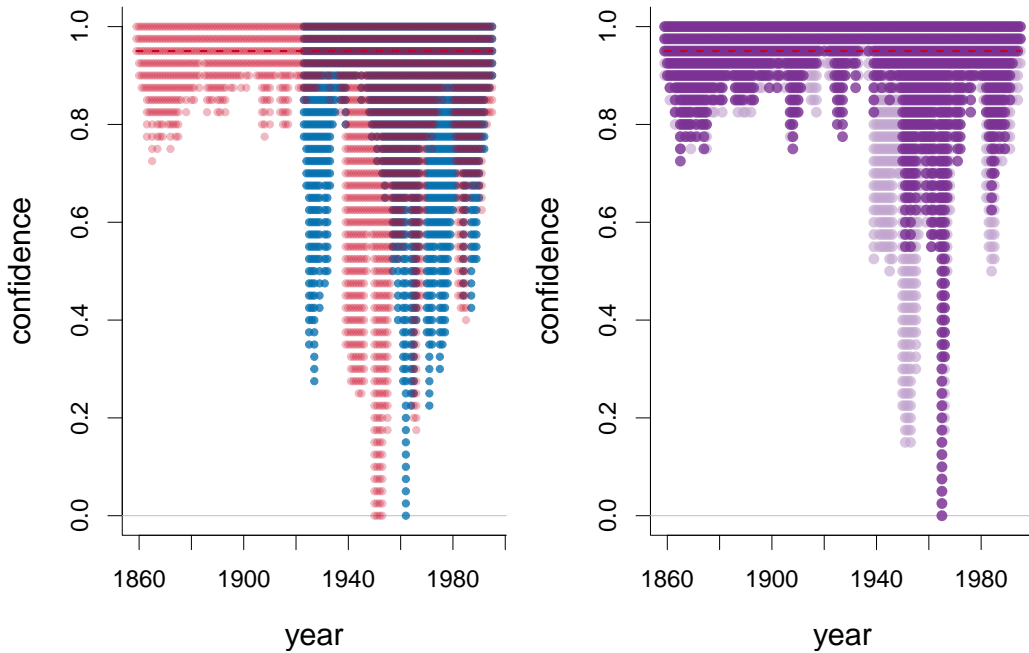


Figure B.2: Left panel: in red the confidence curve based on the battle death data (point estimate 1950), in blue the one based on the Ngram (point estimate 1962). Right panel: combined confidence curves, dark violet with no down-weighting, light violet with down-weighting of the Ngram information. Both these two curves give a point estimate equal to 1965.

We must emphasise that we do not recommend the automatic use of this subjective importance weighting for all or most information combination settings. In usual settings, the ‘degree of informativeness’ of each source is already sufficiently well represented by the likelihood component from that source. However, down-weighting of softer data can be considered in situations like the

present one, with combination of soft and hard data, where there might be stark differences in quality or relevance between the sources.

In this application we have illustrated a situation where one information source was considered to be of higher quality and relevance than the other; a combination of hard and soft data. Note that such combination attempts often require the users to make strong assumptions, for example that very different sources inform on the exact same parameter. Low-quality, large-data sources are expected to play an increasingly important role in statistics in years to come (especially via scraping of the internet). The combination of such data sources with more high-quality sources raises various issues, and we will end with a note of caution. In a best case scenario, the analyst manages to benefit from a large, low-quality source and can obtain more precise statements than those from the smaller, high-quality sources alone. In the worst case scenario, the analyst is contaminating good data with irrelevant noise, and does not learn anything of value.

C Illustration of Cox–Reid in the II step: the Neyman–Scott problem

The Neyman–Scott problem is an extreme example of such a situation. It can be presented of as a meta-analysis problem. We have a large number k of studies, but each study has only two observations (so $n_1 = \dots = n_k = n = 2$). From each source j we observe $y_{i,j} \sim N(\mu_j, \sigma^2)$ where $i = 1, 2$ and $j = 1, \dots, k$. Each sources has a specific mean parameter, but the variance, which is the parameter of main interest, is common across sources. This problem is popular in the literature concerning corrections to the profile likelihood (see e.g. Schweder & Hjort (2016, Ch. 7)), since there exists a simple and exact solution, which serves as a gold standard against which to compare different corrections. We will compare this gold standard solution, as found in Schweder & Hjort (2016, Ch. 4), against the ‘standard’ II-CC-FF solution and the corrected II-CC-FF solution using the simple Cox–Reid correction.

The pivot $\hat{\sigma}^2/\sigma^2$ can be seen to have a $\chi_k^2/(2k)$ distribution, which gives the exact CD,

$$C_{\text{gold}}(\sigma) = 1 - \Gamma_k(2k\hat{\sigma}^2/\sigma^2),$$

where $\Gamma_k(\cdot)$ is the c.d.f. of the χ_k^2 distribution and $\hat{\sigma}^2 = \sum_{j=1}^k S_j^2/(2k) = \sum_{j=1}^k \frac{1}{2}(y_{1,j} - y_{2,j})^2/(2k)$ is the ML estimate (we note that this is a famous case where the ML estimator is inconsistent). The gold standard CD may be turned into a confidence curve using (2.1) and is displayed in black in Figure C.1. For the sake of comparisons, we can write out the confidence likelihood implied by this CD,

$$\ell_{\text{conv,gold}}(\sigma) = -k \log \sigma - \frac{1}{2}(1/\sigma^2) \sum_{j=1}^k S_j^2. \quad (\text{C.1})$$

With the standard II-CC-FF solution we start with the II step where we deal with each source separately: we profile out μ_j and get $\ell_{\text{prof},j}(\sigma) = -2 \log \sigma - \frac{1}{2}(1/\sigma^2)S_j^2$. All the sources inform on exactly the same focus parameter and we can just sum the log-likelihood contributions in the fusion step,

$$\ell_{\text{prof}}(\sigma) = -2k \log \sigma - \frac{1}{2}(1/\sigma^2) \sum_{j=1}^k S_j^2. \quad (\text{C.2})$$

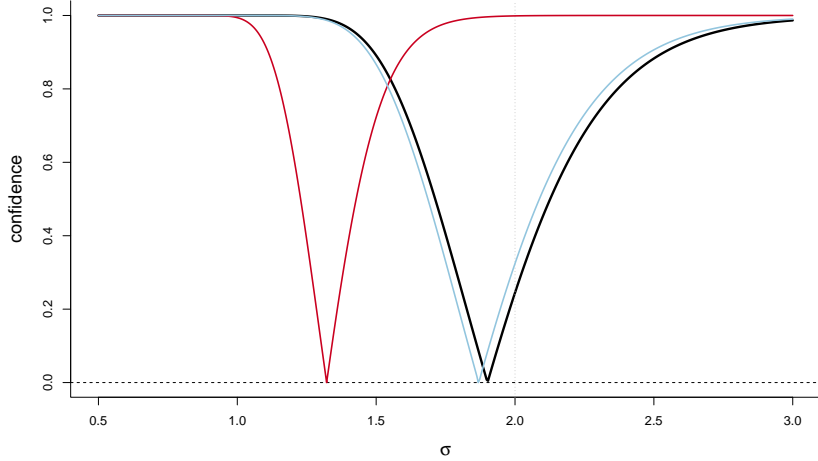


Figure C.1: Neyman–Scott example with $k = 20$ sources, the parameter of main interest $\sigma = 2$, and the source specific means drawn from a uniform between -3 and 3 . The exact confidence curve in black, the standard uncorrected II-CC-FF solution in red, and the corrected II-CC-FF solution in blue.

Comparing this to the confidence log-likelihood for the gold standard in (C.1) we see that they differ by an extra ‘2’ in the first term, which causes the inconsistency of the ML estimator. We may nevertheless construct our confidence curve in the general II-CC-FF manner, $cc_1^*(\sigma, \text{data}) = \Gamma_1(2\{\ell_{\text{prof}}(\hat{\sigma}) - \ell_{\text{prof}}(\sigma)\})$.

For this model, the simple Cox–Reid correction term for each source is $\log \sigma$. The corrected profile log-likelihood for each source is then $\ell_{\text{prof},j}(\sigma) + \log \sigma$, and for the full data we obtain a corrected profile log-likelihood identical to (C.1). Following the II-CC-FF recipe we construct the confidence curve with the Wilks approximation, $cc_2^*(\sigma, \text{data}) = \Gamma_1\{2(\ell_{\text{conv,gold}}(\hat{\sigma}) - \ell_{\text{conv,gold}}(\sigma))\}$.

Figure C.1 gives the three confidence curves in a specific example with $k = 20$ sources. The standard II-CC-FF solution in red is clearly far from the exact black curve. With k increasing, it converges to the wrong value, $\sigma/\sqrt{2}$. The blue curve, on the other hand, corresponding to the II-CC-FF solution with Cox–Reid correction, is close to the exact curve, even though it is constructed using the Wilks approximation. When k increases, for instance to 50, the blue and black curves are virtually identical.